Electronic Supplementary Material (ESI):

Experimental and Theoretical Studies of pH-Responsive Iridium(III) Complexes of Azole and N-Heterocyclic Carbene Ligands

Tahmineh Hashemzadeh,[1] Andrew J Christofferson,[2,3] Keith F. White[1] and Peter J. Barnard[1]*

Department of Biochemistry and Chemistry, La Trobe Institute for Molecular Science, La Trobe University, Victoria, 3086, Australia, E-mail: p.barnard@latrobe.edu.au

School of Science, STEM College, RMIT University, Melbourne, Victoria 3001, Australia

ARC Centre of Excellence in Exciton Science, School of Science, RMIT University, Melbourne, Victoria 3001, Australia

Table of contents

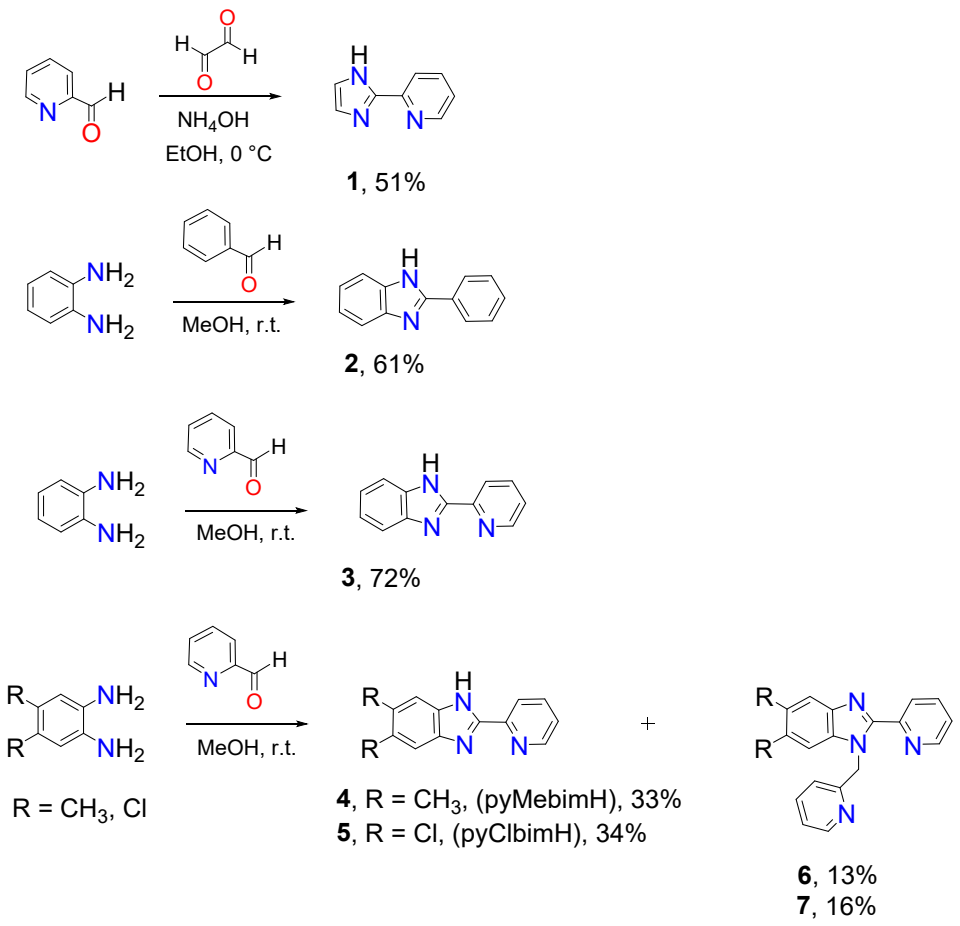

Scheme S1. Preparation of (pyimH) **1**, (pybimH) **2** and (phbimH) **3,** (pyMebimH) **4**, (pyClbimH) **5**, **6** and **7**.

1. Synthesis

$[Ir(ppy)_2Cl]_2$. This compound was prepared as described previously.[1] To a solution of $IrCl_3.xH_2O$ (1.02 g, 3.42 mmol) in distilled 2-ethoxy ethanol (60 mL) and distilled water (20 mL) was added 2-phenylpyridine (1.2 mL, 8.54 mmol). The mixture was heated at 120 °C under a nitrogen atmosphere. A yellow precipitate appeared after 2 h. The reaction was continued for 16 h and after cooling the resulting yellow crystals were collected and washed with water and ether. (yield 1.49 g, 81%).

^{1}H NMR (500 MHz, d_6-DMSO): δ= 6.25 (d, J = 7.37 Hz, 1 H), 5.66 (d, J = 7.37 Hz, 1 H), 6.70 (t, J = 7.63Hz, 1H), 6.76 (t, J = 7.63 Hz, 1H), 6.84 (t, J = 7.63 Hz, 1H), 6.89 (t, J = 7.63 Hz, 1H), 7.45 (t, J = 6.80 Hz, 1H), 7.57 (t, J = 6.80 Hz, 1H), 7.73 (d, J = 7.40 Hz, 1H), 7.78 (d, J = 7.40 Hz, 1H), 8.00 (t, J = 7.77 Hz, 1H), 8.09 (t, J = 7.77 Hz, 1H), 8.18 (d, J = 8.03 Hz, 1H), 8.26 (d, J = 8.03 Hz, 1H), 9.54 (d, J = 5.19 Hz, 1H), 9.80 (d, J = 5.60 Hz, 1H) ppm. ^{13}C NMR (500 MHz, d_6-DMSO): δ= 120.0, 120.5, 122.6,

122.9, 123.3, 124.0, 124.3, 125.2, 129.5, 130.0, 130.4, 131.7, 138.8, 139.8, 143.6, 144.1, 145.4, 151.0, 152.3, 152.5, 167.3, 167.7 ppm.

$[Ir(phbim)_2Cl]_2$. This compound was prepared as described for $[Ir(ppy)_2Cl]_2$ from $IrCl_3.xH_2O$ (0.30 g, 1.00 mmol), (0.4 g, 2.00 mmol) of 2-phenylbenzimidazole **2** in a mixture of 28 mL of 2-ethoxy ethanol and water 3:1 (v/v). The product was obtained as a green solid after the addition of water. (yield 0.48 g, 78%).

^{1}H NMR (500 MHz, d_6-DMSO): δ= 5.76 (d, J = 7.01 Hz, 1H), 6.35 (d, J = 6.62 Hz, 1H), 6.64 (d, J = 10.2 Hz, 2H), 6.86 (d, J = 8.00 Hz, 2H), 7.32-7.34 (m, 2H), 7.39-7.41 (m, 2H), 7.66-7.71(m, 4H), 8.62 (d, J = 7.65 Hz, 1H), 8.77 (d, J = 7.46 Hz, 1H), 13.67 (s, 1H), 13.87 (s, 1H) ppm. ^{13}C NMR (500 MHz, d_6-DMSO): δ= 112.5, 113.0, 117.7, 118.4, 121.8, 122.5, 123.2, 123.4, 123.6, 123.7, 123.8, 124.2, 129.5, 130.3, 131.6, 133.6, 134.0, 134.1, 134.2, 134.7, 140.6, 141.4, 144.7, 152.9, 164.3, 165.1 ppm.

1. This compound was prepared as described previously.[2] An ice-cold solution of 2-pyridinecarboxyaldehyde (20 g, 186.72 mmol) in 25 mL ethanol was added to an ice-cold solution of 40% aqueous glyoxal (27 mL) in 10 mL ethanol, and then ice-cold concentrated aqueous NH_4OH solution (64 mL) was added immediately. This solution was stirred at 0 °C for 1 h, and then warmed to room temperature (RT), and stirred for an additional 5 h. The volatiles were evaporated under reduced pressure and the residue was then extracted six times with diethyl ether (500 mL) which gave **1** as a brown crystalline solid. (yield 13.91 g, 51%).

^{1}H NMR (500 MHz, d_6-DMSO): δ= 7.08 (s, 1 H, ImH), 7.22 (s, 1 H, ImH), 7.33 (t, 3JHH= 6.19 Hz, 1 H, PyH), 7.86 (t, J = 7.83 Hz, 1 H, PyH), 8.04 (d, J = 7.91 Hz, 1 H, PyH), 8.57 (d, J = 4.81 Hz, 1 H, PyH), 12.78 (s, 1 H, NH) ppm. ^{13}C NMR (500 MHz, d_6-DMSO): δ =118.7, 119.4, 122.9, 129.5, 137.2, 145.6, 148.9, 149.0 ppm.

2. This compound was prepared as described previously.[3, 4] In a 250 mL Schlenk flask under a nitrogen atmosphere a mixture of o-phenylenediamine (1 g, 9.25 mmol), Na_2SO_4 (1.97 g, 13.87 mmol) and benzaldehyde (1.96 g, 18.49 mmol). Compound **2** was obtained as light brown crystals. (yield 1.1 g, 61%).

^{1}H NMR (500 MHz, d_6-DMSO): δ= 7.19-7.21 (m, 2 H), 7.47-7.60 (m, 5 H), 8.18 (d, J = 7.20 Hz, 2 H), 12.91 (b, 1 H, NH) ppm. ^{13}C NMR (500 MHz, d_6-DMSO): δ =122.7, 126.8, 129.4, 130.2, 130.4, 151.7 ppm.

3. This compound was prepared as described for **2** from o-phenylenediamine (1 g, 9.25 mmol), and Na_2SO_4 (1.97 g, 13.87 mmol) in 20 mL dry methanol was prepared. 2-pyridinecarboxaldehyde (1.98 g, 18.49 mmol) in 40 mL of dry methanol was added dropwise and the resulting mixture was stirred at RT, overnight. Then the solution was filtered, and the volatiles were evaporated from the filtrate under reduced pressure yielding a sticky brown solid. This crude compound was suspended in hot acetonitrile and after cooling at RT, the product crystalized and was collected and washed with hexane, yielding **3** as a light brown crystalline solid. (yield 1.3 g, 72%).

^{1}H NMR (500 MHz, d_6-DMSO): δ= 7.22 (t, J = 6.27 Hz, 2 H, PhH), 7.49-7.68 (m, 3 H), 7.99-8.03 (m, 1 H), 8.32-8.35 (m, 1 H), 8.74-8.76 (m, 1 H), 13.08 (s, 1 H, NH) ppm. ^{13}C NMR (500 MHz, d6-DMSO): δ =112.0, 119.3, 121.4, 121.9, 123.0, 124.7, 134.9, 137.5, 144.0, 148.5, 149.4, 150.7 ppm.

4 and **6**. These compounds were prepared as described for **3** from of 4,5-dimethyl-1,2 phenylenediamine (1 g, 7.34 mmol), Na_2SO_4 (1.56 g, 11.01 mmol) and 2-pyridinecarboxaldehyde (1.57 g, 14.68 mmol). The products were purified on silica with hexane and ethyl acetate (9:1 v/v) as the eluent and two compound containing fractions were collected. After removal of the solvent compounds **4** and **6** were obtained as orange solids (yield 0.54 g, 33% and yield 0.31 g, 13% respectively).

^{1}H NMR (400 MHz, d_6-DMSO): δ= 2.32 (s, 6 H, CH_3), 7.30-7.49 (m, 3 H), 7.96 (t, J = 7.73 Hz, 1 H, PyH), 8.26-8.28 (m, 1 H), 8.69-8.70 (m, 1 H), 12.83 (s, 1 H, NH) ppm. ^{13}C NMR (400 MHz, d_6-DMSO): δ =20.04, 111.9, 119.2, 121.1, 124.3, 130.3, 131.9, 133.5, 137.4, 142.6, 148.8, 149.2, 149.9 ppm.

6. ^{1}H NMR (400 MHz, d_6-DMSO): δ= 2.28 (s, 3 H, CH_3), 2.32 (s, 3 H, CH_3), 6.23 (s, 2 H, CH_2), 6.94 (d, J = 7.87 Hz, 1 H, PyH), 7.17-7.20 (m, 1 H), 7.29 (s, 1 H, PhH), 7.40-7.43 (m, 1 H), 7.52 (s, 1 H, PhH), 7.63 (t, J = 7.44 Hz, 1 H, PyH), 7.94 (t, J = 7.78 Hz, 1 H, PyH), 8.33 (d, J = 8.09 Hz, 1 H, PyH), 8.41 (d, J = 4.26 Hz, 1 H, PyH), 8.57 (d, J = 4.73 Hz, 1 H, PyH) ppm. ^{13}C NMR (400 MHz, d6-DMSO): δ =19.9, 20.2, 49.9, 111.0, 119.5, 120.7, 122.3, 123.9, 124.0, 131.1, 132.3, 135.4, 136.9, 137.3, 140.9, 148.5, 148.6, 149.1, 150.2, 157.1 ppm.

5 and **7**. This compound was prepared as described for **3** from 4,5-dichloro-o-phenylenediamine (1.25 g, 7.06 mmol), Na_2SO_4 (1.50 g, 10.60 mmol) and 2-pyridinecarboxaldehyde (1.51 g, 14.12 mmol). Compounds **5** and **7** were obtained as pale-purple solids. (yield 0.64 g, 34% and yield 0.41 g, 16% respectively).

^{1}H NMR (400 MHz, d_6-DMSO): δ=7.56 (t, J = 6.31 Hz, 1 H, PyH), 7.85 (br. s, 2H, PhH), 8.02 (t, J = 8.05 Hz, 1 H, PyH), 8.31 (d, J = 7.85 Hz, 1 H, PyH), 8.75 (d, J = 4.42 Hz, 1 H, PyH), 13.37 (s, 1 H, NH)

ppm. ^{13}C NMR (400 MHz, d_6-DMSO): δ =113.1, 113.3, 120.5, 120.6, 121.8, 125.3, 134.5, 137.7, 143.5, 147.6, 149.6, 153.1 ppm.

7. ^{1}H NMR (400 MHz, d_6-DMSO): δ=6.28 (s, 2 H, CH_2), 7.18-7.21 (m, 2 H), 7.46-7.49 (m, 1 H), 7.69 (t, J = 7.69 Hz, 1 H, PyH), 7.96-8.00 (m, 3 H), 8.32-8.36 (m, 2 H), 8.62 (d, J = 2.57 Hz, 1 H, PyH) ppm. ^{13}C NMR (400 MHz, d_6-DMSO): δ =50.0, 113.1, 120.6, 121.3, 122.5, 124.4, 124.8, 125.1, 125.8, 136.7, 136.9, 137.6, 141.6, 148.8, 149.1, 149.2, 151.8, 156.2 ppm.

8. This compound was prepared as described previously.[5] A solution of 2-bromopyridine (5.0 g, 31.64 mmol), CuI (0.55 g, 2.88 mmol), L-proline (0.66 g, 5.75 mmol), imidazole (1.96 g, 28.77 mmol) and K_2CO_3 (7.95 g, 57.53 mmol) in 30 mL of DMSO was heated at 60 °C under an atmosphere of nitrogen for 72 h. The cooled mixture was partitioned between water and ethyl acetate (3×50 mL) and the combined organic layers were washed with brine and dried with Na_2SO_4 and the volatiles were evaporated under reduced pressure. The residual oil was purified on silica with hexane and ethyl acetate (9:1 v/v) as the eluent. The product containing fractions were evaporated under reduced pressure and drying the residue in vacuo gave **8** as yellow liquid. (yield 2.62 g, 63%).

^{1}H NMR (500 MHz, d_6-DMSO): δ= 7.13 (d, 3JHH= 1.17 Hz, 1 H, ImH), 7.33-7.36 (m, 1 H), 7.80 (d, J = 8.24 Hz, 1 H, PyH), 7.94-7.99 (m, 2 H), 8.48 (d, J = 3.32 Hz, 1 H, PyH), 8.54 (d, J = 0.91 Hz, 1 H, ImH) ppm. ^{13}C NMR (500 MHz, d_6-DMSO): δ =112.7, 116.5, 122.2, 130.1, 135.0, 140.0, 148.6, 148.8 ppm.

9. This compound was prepared as described for **8**, from 2-bromopyridine (5.3 g, 33.42 mmol), copper iodide (0.58 g, 3.04 mmol), L-proline (0.7 g, 6.08 mmol), 1,2-4 triazole (2.1 g, 30.38 mmol) and potassium carbonate (8.4 g, 60.8 mmol). After removal of the volatiles under reduced pressure the residue was recrystallized from hexane which gave the corresponding coupling product **9** as pure white crystalline solid. (yield 2.93 g, 66%).

^{1}H NMR (400 MHz, d_6-DMSO): δ= 7.48 (t, J = 5.87 Hz, 1 H, PyH), 7.86-7.88 (m, 1 H, PyH), 8.07 (t, J = 8.21 Hz, 1 H, PyH), 8.30 (s, 1 H, trzH), 8.54 (d, J = 4.85 Hz, 1 H, PyH), 9.37 (s, 1 H, trzH) ppm. ^{13}C NMR (400 MHz, d_6-DMSO): δ =113.4, 124.1, 140.6, 142.4, 149.1, 153.5. ppm.

10. To a solution of **8** (0.42 g, 2.91 mmol) in 10 mL acetonitrile was added methyl iodide (0.5 g, 3.52 mmol). The colourless solution was then heated at reflux for 24 h and after cooling, the solvent was evaporated under reduced pressure and the resulting pale-yellow solid was recrystallized from ethanol and washed with ether which gave **10** as a white crystalline solid. (yield 0.61 g, 73%).

^{1}H NMR (500 MHz, d_6-DMSO): δ= 3.97 (s, 3 H, CH_3), 7.64 (t, J = 6.26 Hz, 1 H, PyH), 7.96 (t, J = 1.81 Hz, 1 H, PyH), 8.00 (d, J = 8.15 Hz, 1 H, ImH), 8.22 (t, J = 8.30 Hz, 1 H, PyH), 8.50 (t, J = 1.79 Hz, 1 H, PyH), 8.65 (d, J = 5.01 Hz, 1 H, ImH), 10.03 (s, 1 H, ImH) ppm. ^{13}C NMR (500 MHz, d_6-DMSO): δ =36.4, 114.1, 119.0, 124.8, 125.2, 135.5, 140.6, 146.4, 149.2 ppm.

11. This compound was prepared as described for **10**, from **9** (0.39 g, 2.65 mmol) and methyl iodide (0.45 g, 3.18 mmol). Compound **11** was obtained as a white crystalline solid. (yield 0.65 g, 85%).

^{1}H NMR (500 MHz, d_6-DMSO): δ= 3.99 (s, 3 H, CH_3), 7.69 (t, J = 6.18 Hz, 1 H, PyH), 8.02-8.04 (m, 1 H, PyH), 8.22 (t, J = 7.89 Hz, 1 H, PyH), 8.66 (d, J = 4.84 Hz, 1 H, PyH), 9.33 (s, 1 H, trzH), 10.91 (s, 1 H, trzH) ppm. ^{13}C NMR (500 MHz, d_6-DMSO): δ =35.0, 114.2, 126.6, 141.5, 142.1, 146.7, 147.4, 149.7 ppm.

2. **High Resolution Mass Spectra for iridium(III) complexes**

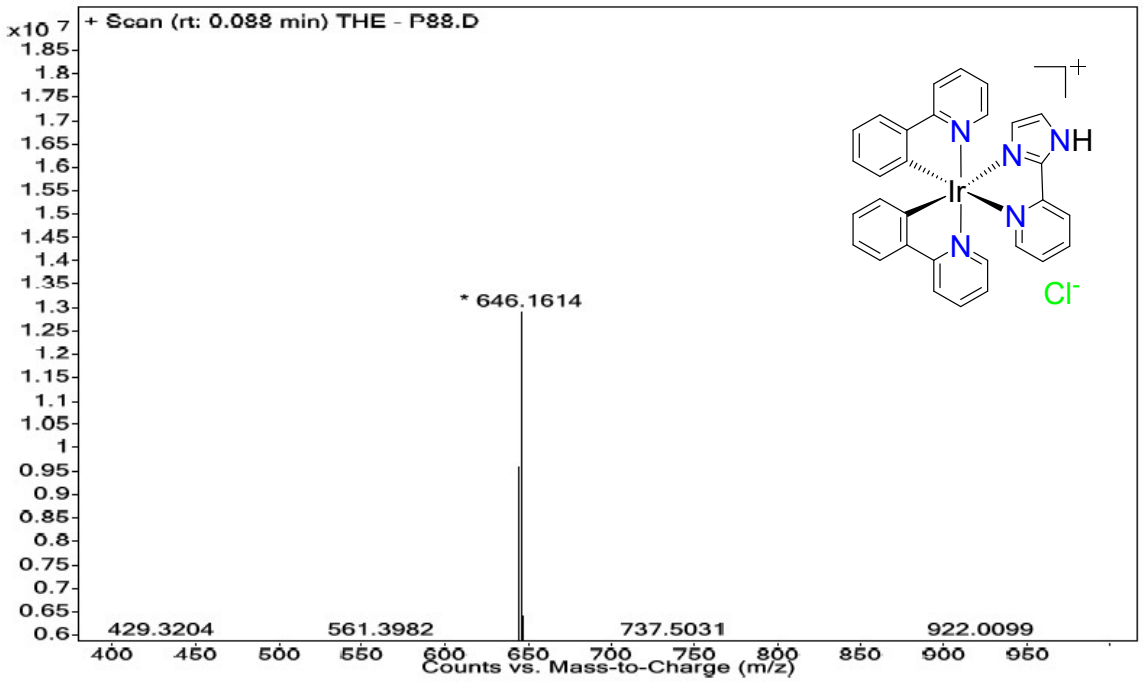

Figure S1. HRMS spectrum of **12** in CH_3OH.

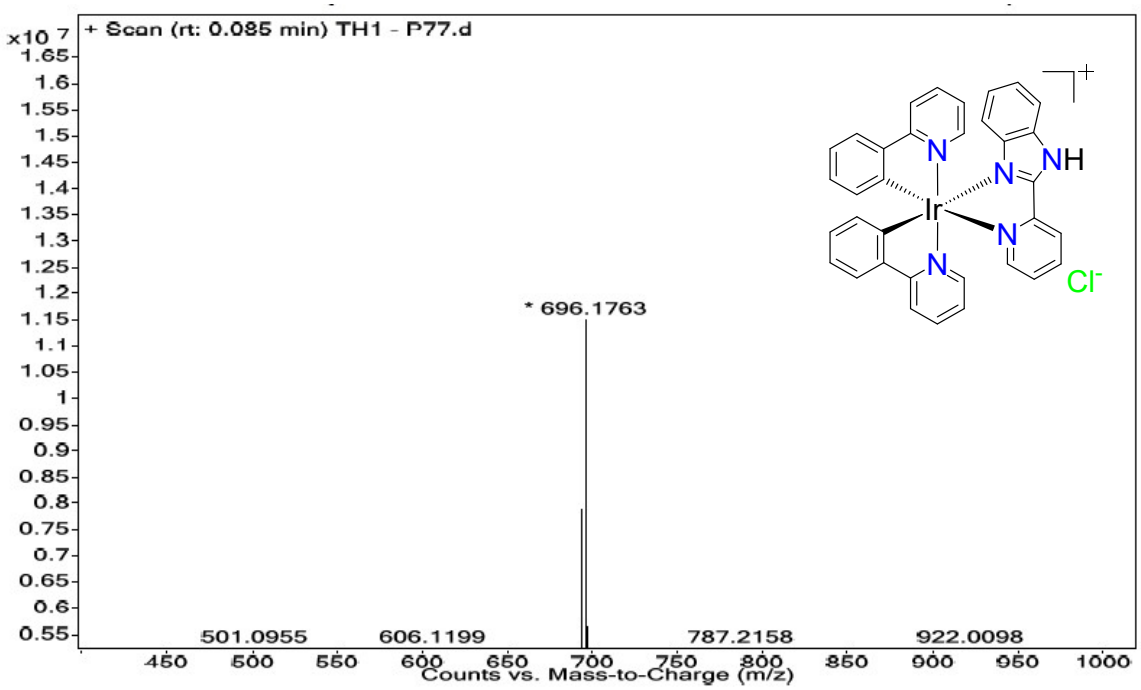

Figure S2. HRMS spectrum of **13** in CH_3OH.

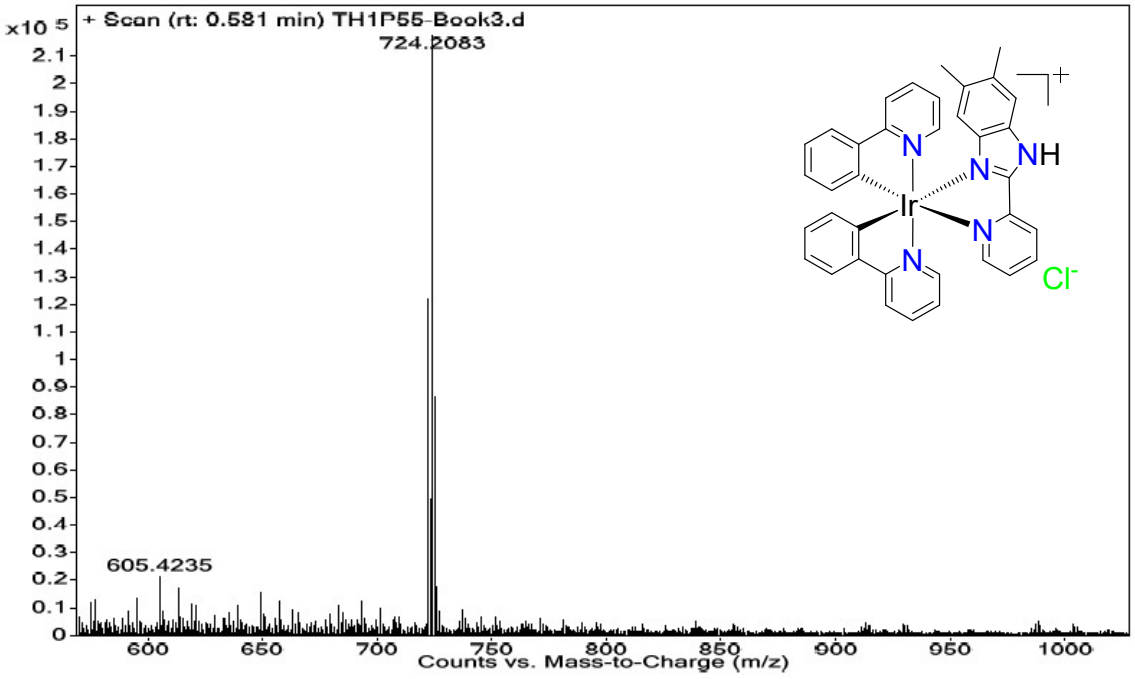

Figure S3. HRMS spectrum of **14** in CH_3OH.

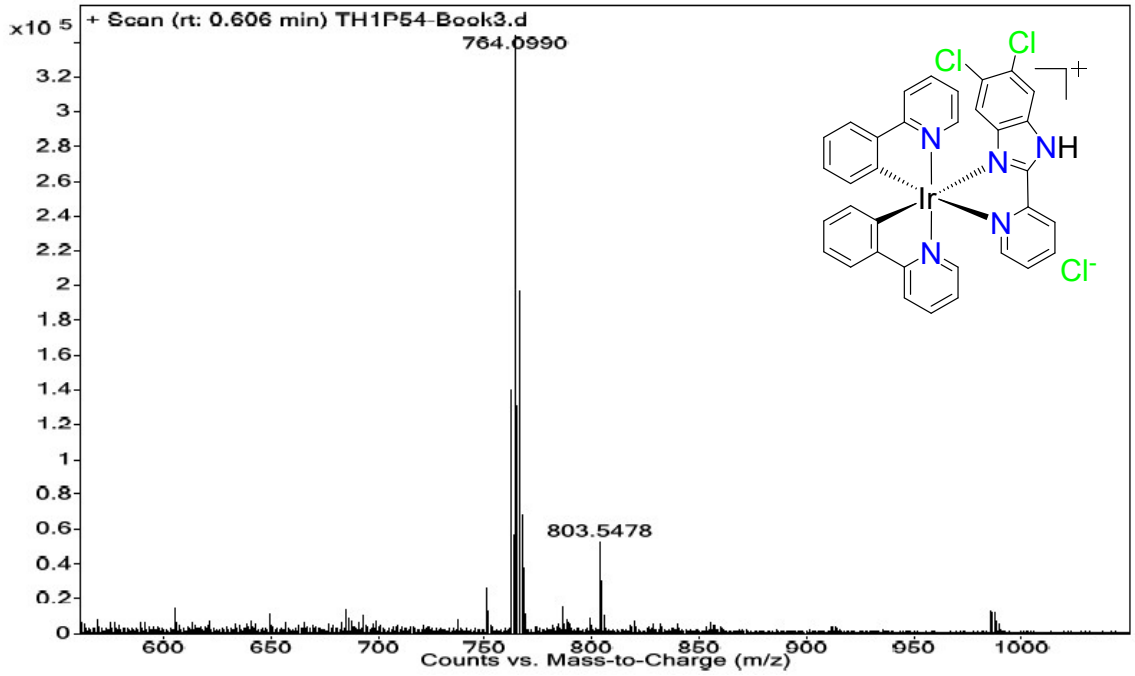

Figure S4. HRMS spectrum of **15** in CH_3OH.

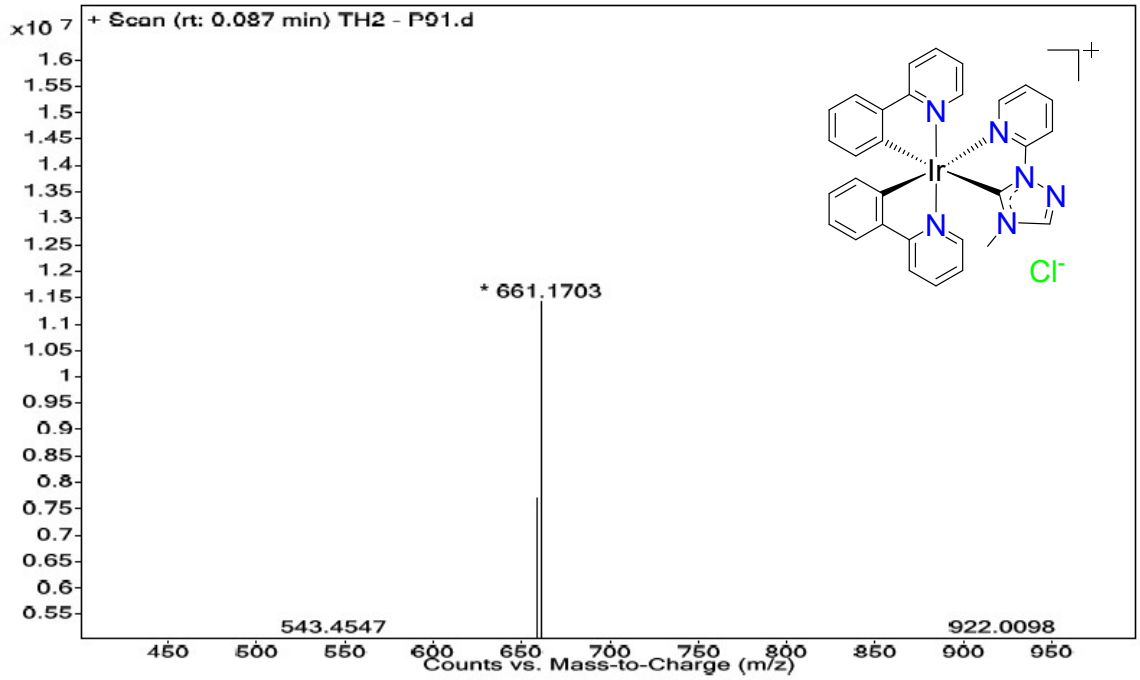

Figure S5. HRMS spectrum of **16** in CH_3OH.

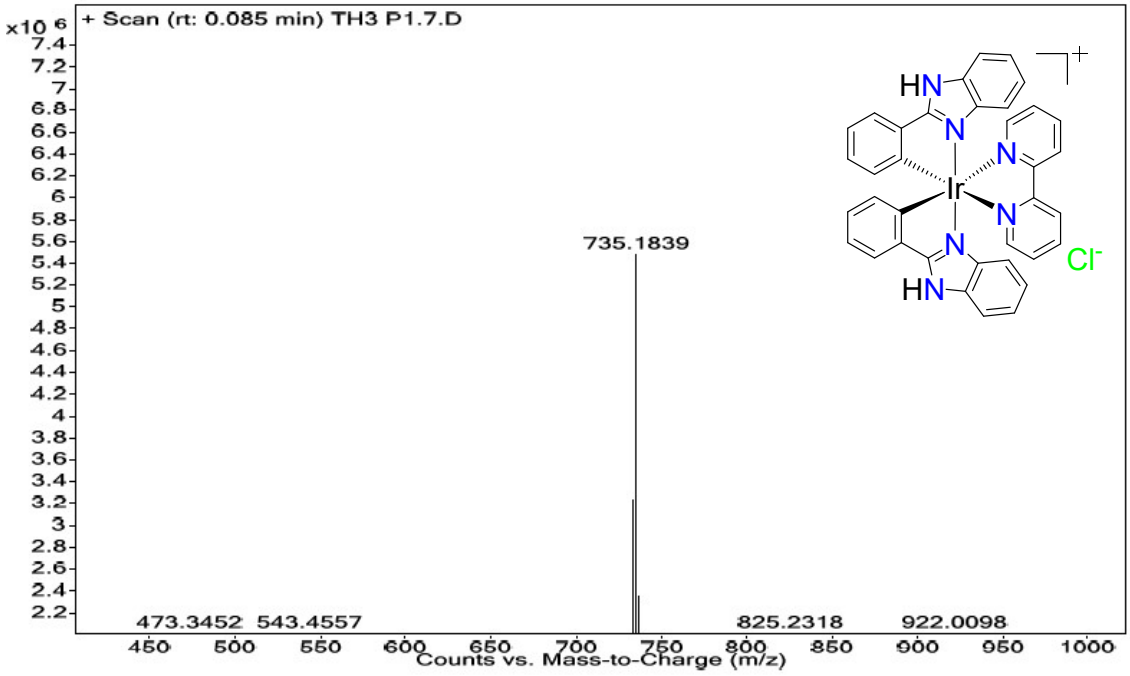

Figure S6. HRMS spectrum of **17** in CH_3OH.

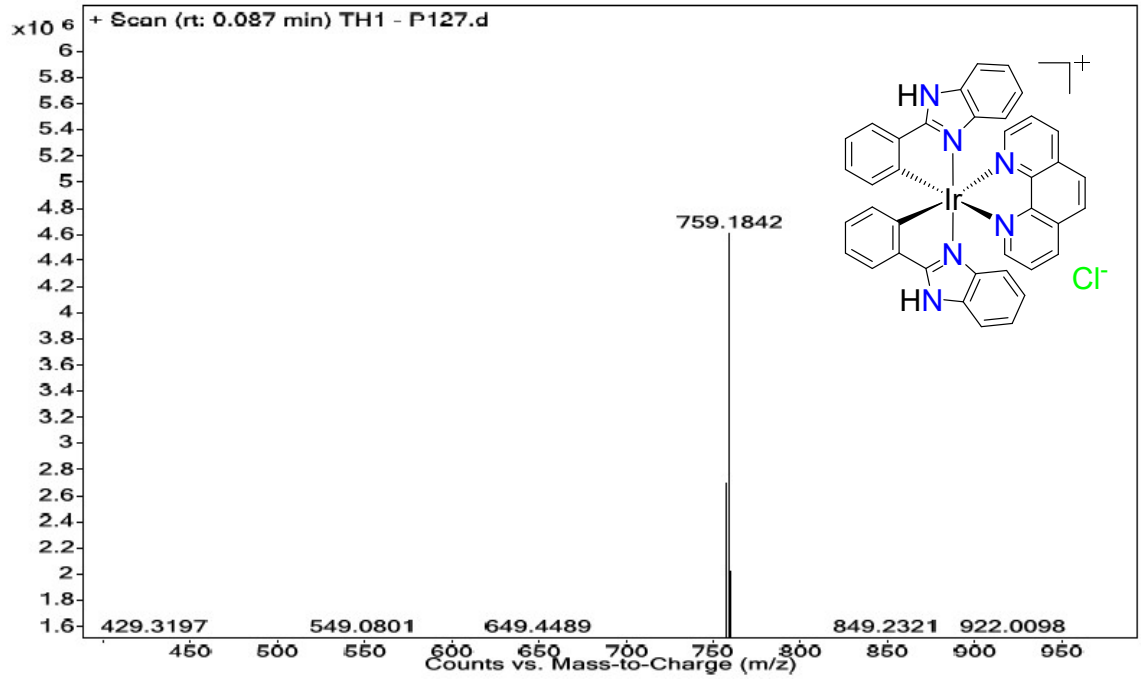

Figure S7. HRMS spectrum of **18** in CH_3OH.

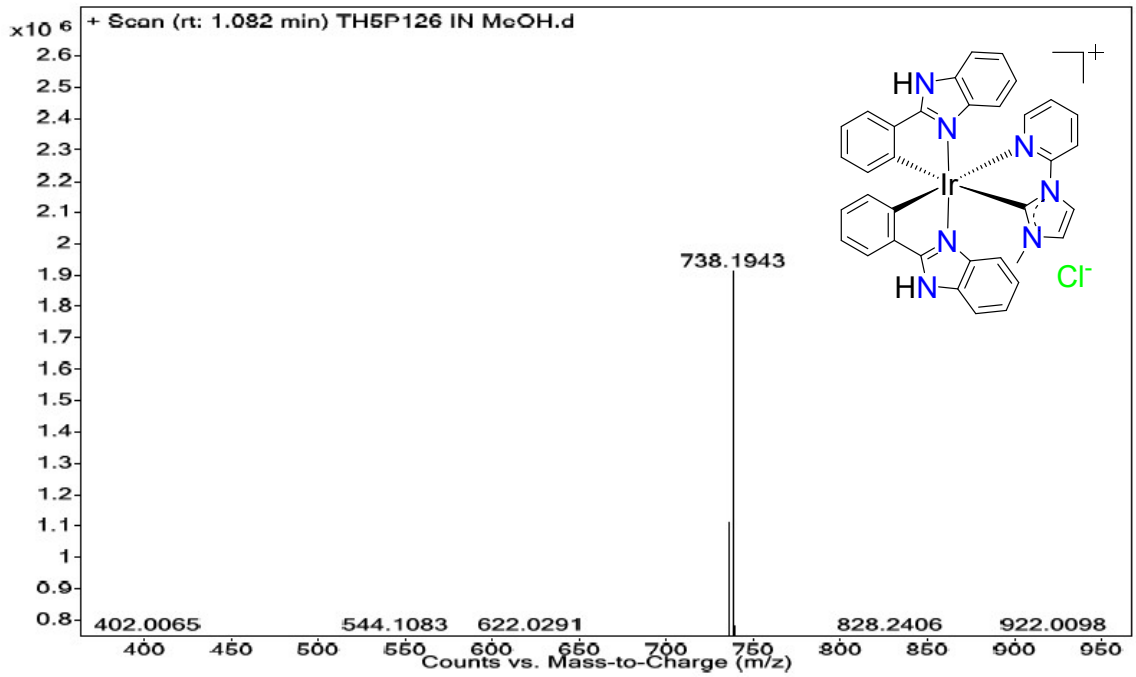

Figure S8. HRMS spectrum of **19** in CH_3OH.

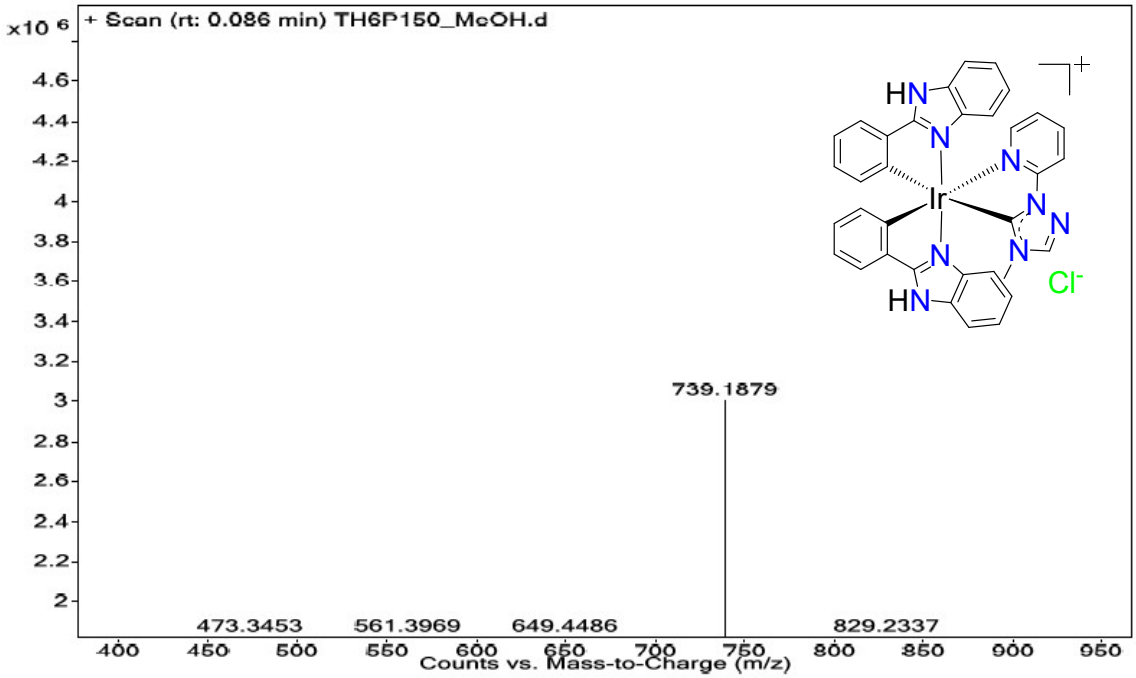

Figure S9. HRMS spectrum of **20** in CH_3OH.

3. X-Ray Crystallography

Table S1. Summary of crystallographic data for complexes **13**, **14**, **16**, **17** and **18**.

Compound	**13**	**14**	**16**	**17**	**18**
Empirical formula	$C_{34}H_{31}ClIrN_5O_3$	$C_{37}H_{36}ClIrN_5O_{2.5}$	$C_{32}H_{27}ClIrN_7$	$C_{40}H_{36}ClIrN_6O$	$C_{44}H_{41}ClIrN_6O_{1.5}$
Formula weight	785.33	818.36	737.25	844.40	905.48
Temperature/K	159(4)	150(1)	180(4)	150(1)	150(1)
Crystal system	monoclinic	tetragonal	monoclinic	orthorhombic	monoclinic
Space group	$P2_1/c$	$P\bar{4}b2$	$P2_1/c$	$Pca2_1$	$C2/c$
a/Å	9.2393(2)	28.0735(4)	8.6419(1)	17.64348(9)	25.9468(6)
b/Å	28.2368(3)		32.2748(5)	8.66040(4)	13.8283(2)
c/Å	16.1627(4)	8.9606(2)	10.5786(2)	22.95688(13)	24.2672(5)
α/°					
β/°	132.839(4)		99.392(2)		112.536(3)
γ/°					
Volume/Å^3	3091.9(2)	7062.0(3)	2910.98(8)	3507.80(3)	8042.2(3)
Z	4	8	4	4	8
ρ_{calc}g/cm^3	1.687	1.539	1.682	1.599	1.496
μ/mm^{-1}	9.508	3.897	9.996	8.393	7.373
F(000)	1552.0	3256.0	1448.0	1680.0	3624.0
Crystal size/mm^3	0.08 x 0.02 x 0.02	0.24 × 0.17 × 0.08	0.33 × 0.11 × 0.06	0.07 × 0.05 × 0.03	0.21 × 0.2 × 0.09
Radiation	Cu$K\alpha$ (λ = 1.54184)	Mo $K\alpha$ (λ = 0.71073)	Cu $K\alpha$ (λ = 1.54184)	Cu$K\alpha$ (λ = 1.54184)	Cu $K\alpha$ (λ = 1.54184)
2Θ range for data collection/°	8.09 to 142.48	6.46 to 56.834	8.904 to 137.144	7.702 to 139.712	7.378 to 136.962
Index ranges	-11 ≤ h ≤ 8, -34 ≤ k ≤ 34, -15 ≤ l ≤ 19	-36 ≤ h ≤ 36, -37 ≤ k ≤ 35, -11 ≤ l ≤ 11	-10 ≤ h ≤ 10, -38 ≤ k ≤ 35, -12 ≤ l ≤ 12	-20 ≤ h ≤ 21, -10 ≤ k ≤ 10, -27 ≤ l ≤ 27	-31 ≤ h ≤ 31, -12 ≤ k ≤ 16, -28 ≤ l ≤ 29
Reflections collected	30795	91934	53765	68323	40499
Independent reflections	5812 R_{int} = 0.0338, R_{sigma} = 0.0196]	8552 [R_{int} = 0.1938, R_{sigma} = 0.0813]	5339 [R_{int} = 0.0508, R_{sigma} = 0.0160]	6486 [R_{int} = 0.0315, R_{sigma} = 0.0129]	7342 [R_{int} = 0.0382, R_{sigma} = 0.0213]
Data/restraints/parameters	5812/0/382	8552/0/391	5339/0/372	6486/1/445	7342/0/415
Goodness-of-fit on F^2	1.090	1.030	1.183	1.038	1.115
Final R indexes [I>=2σ (I)]	R_1 = 0.0291, wR_2 = 0.0686	R_1 = 0.0534, wR_2 = 0.1217	R_1 = 0.0340, wR_2 = 0.0814	R_1 = 0.0199, wR_2 = 0.0514	R_1 = 0.0531, wR_2 = 0.1443
Final R indexes [all data]	R_1 = 0.0297, wR_2 = 0.0686	R_1 = 0.0715, wR_2 = 0.1282	R_1 = 0.0345, wR_2 = 0.0818	R_1 = 0.0200, wR_2 = 0.0515	R_1 = 0.0548, wR_2 = 0.1469
Largest diff. peak/hole/ e Å^{-3}	2.41/-1.00	0.97/-0.65	2.30/-1.36	1.31/-0.77	6.88/-2.27
Flack parameter		0.045(12)		-0.028(3)	

13, X-ray data was collected on a Rigaku Supernova diffractometer using a Cu$K\alpha$ radiation source. The crystal was kept at a steady, T = 159 K, during data collection. A multi-scan absorption correction was applied using CrysAlisPro 1.171.40.53 (Rigaku Oxford Diffraction, 2019). A solution was found in the monoclinic space group $P2_1/c$. All Ir(III)-complex, chloride counter ion and solvent atoms were clearly defined and modelled using anisotropic displacement parameters. All hydrogens were placed at

geometrically estimated positions. Electron density attributed to solvent could not be satisfactorily modelled. A solvent mask was calculated and 12 electrons per unit cell was found, consistent with one water molecule, and removed from the data set.

14, X-ray data was collected on a Rigaku Supernova diffractometer using a Mo*Kα* radiation source. The crystal was kept at a steady, T = 150 K, during data collection. A Gaussian absorption correction was applied using CrysAlisPro 1.171.40.53 (Rigaku Oxford Diffraction, 2019). The X-ray data indicated missing reflections at low angles this is, likely a result of beam-stop interference occurring through the use of Mo radiation and a crystal with a large unit cell. The number of unique reflections used in the analysis was 8552. A systematic analysis of the data for the space group found the best fit to be for the tetragonal space group $P\bar{4}b2$, an R_{int} value of 0.19 is likely a result of the missing reflections. All Ir(III) complex and chloride counter ion atoms were well defined and modelled with anisotropic displacement parameters. Hydrogen atoms were placed at geometrically estimated positions. Solvent molecules could not be satisfactorily modelled. A solvent mask calculated and removed from the data set, 32e^- (volume 194 Å^3) per asymmetric unit, consistent with 1 MeOH and 1.5 H_2O molecules.

16, X-ray data was collected on a Rigaku Supernova diffractometer using a Cu*Kα* radiation source. A Gaussian absorption correction was applied using CrysAlisPro 1.171.40.53 (Rigaku Oxford Diffraction, 2019). A solution was found in the monoclinic space group $P2_1/c$. All Ir(III)-complex, chloride counter ion and solvent atoms were clearly defined and modelled using anisotropic displacement parameters. All hydrogens were placed at geometrically estimated positions.

17, X-ray data was collected on a Rigaku Supernova diffractometer using a Cu*Kα* radiation source. The crystal was kept at a steady, T = 150 K, during data collection. A multi-scan absorption correction was applied using CrysAlisPro 1.171.40.53 (Rigaku Oxford Diffraction, 2019). A solution was found in the orthorhombic space group $Pca2_1$. All Ir(III)-complex, chloride counter ion and diethyl ether solvent atoms were clearly defined and modelled using anisotropic displacement parameters. All hydrogens were placed at geometrically estimated positions.

18, X-ray data was collected on a Rigaku Supernova diffractometer using a Cu*Kα* radiation source. A solution was found in the monoclinic space group $C2/c$. A multi-scan absorption correction was applied using CrysAlisPro 1.171.40.53 (Rigaku Oxford Diffraction, 2019). The Ir(III) complex and chloride counterion atoms were clearly defined and refined with anisotropic displacement parameters, hydrogen atoms were placed at geometrically estimated positions. Electron density attributed to disordered diethyl ether could not be satisfactorily modelled, a solvent mask was calculated and 66 e^- per unit asymmetric,

consistent with 1.5 molecules of diethyl ether, was removed from the data set. Unaccounted for, large peaks of electron density remain in the model. The peaks reside close to the heavy Ir(III) cation. Attempts to perform face absorption corrections resulted in a very low data/parameter ratio and unstable refinement and were not applied in the final HKL file.

4. UV-visible pH Titration Studies for complexes 12-15 and 17-20

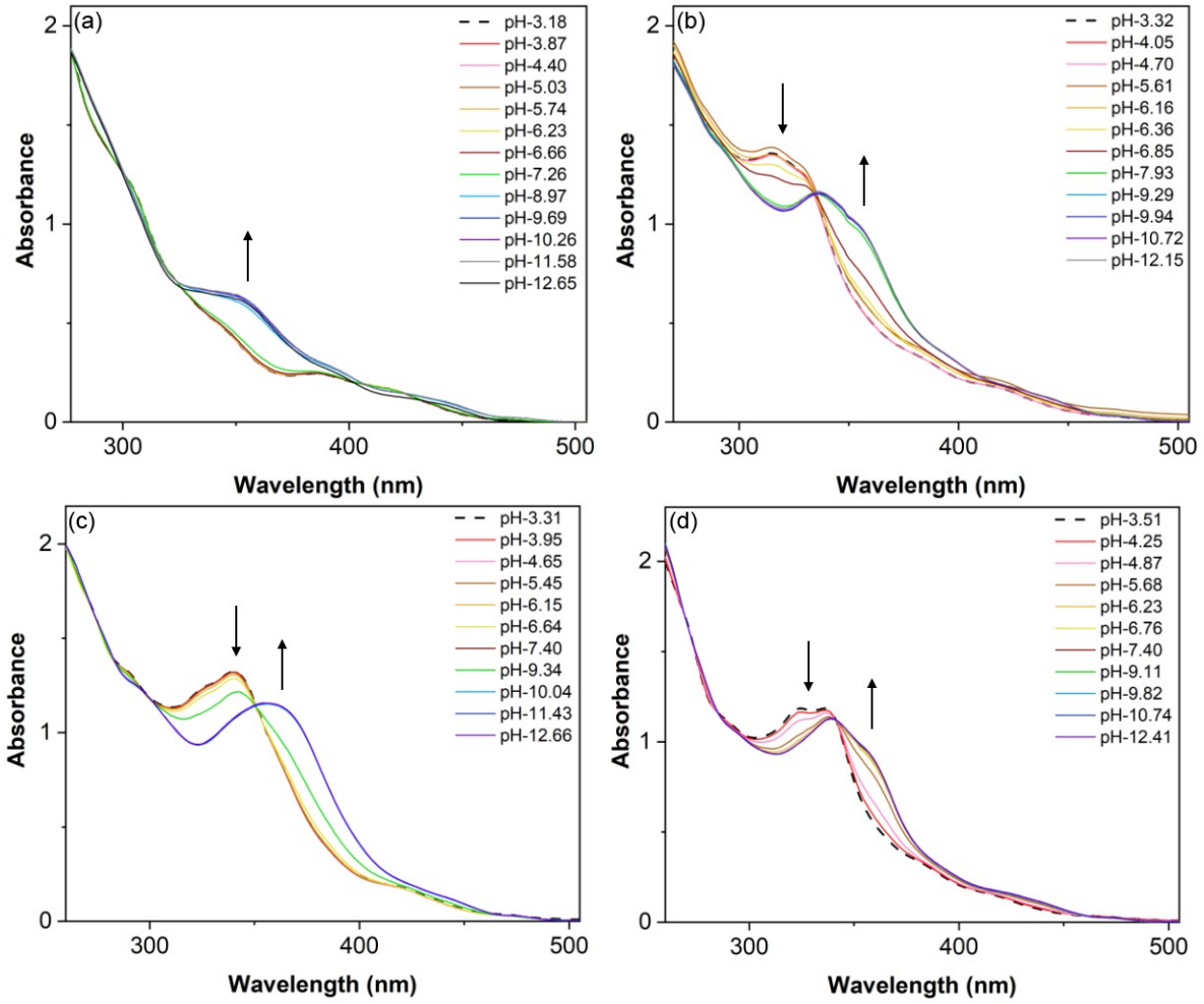

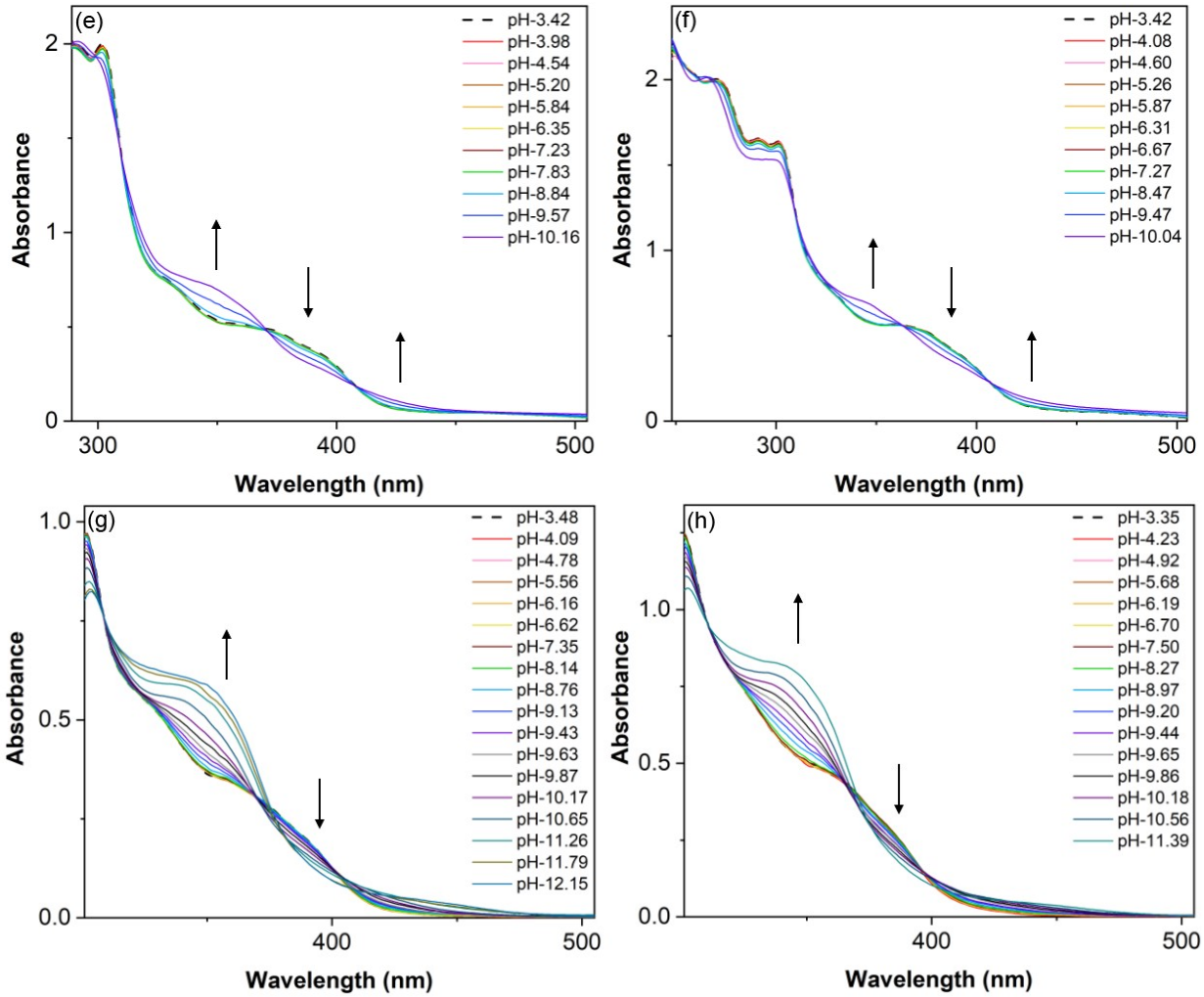

Figure S10. UV-vis absorption spectra of (a) **12**, (b) **13**, (c) **14**, (d) **15,** (e) **17,** (f) **18,** (g) **19** and (h) **20** recorded as a function of pH in a mixture of 1:1 BR buffer and DMSO. [Complex] = 50 μM, [BR buffer] = 20 mM. The pH was adjusted with additions of 2 μL 6 M NaOH.

5. pK_a Calculations and Computational Results

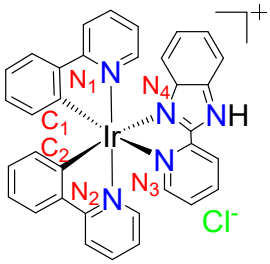

Figure S11. Molecular structure of complex **13** with atom numbering scheme, which was used as a benchmark to determine the appropriate functional for DFT calculation.

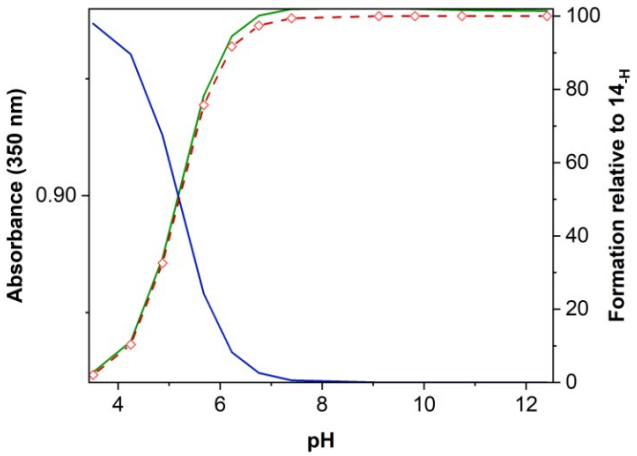

Figure S12. HypSpec 2014 calculated concentration distribution curves for the equilibria species relative to the total complex concentration of **14**. The red diamonds indicate the experimental absorbance (350 nm) values, and the red dashed line represents the calculated curve for absorbance at 350 nm relative to solution pH. The solution speciation (concentrations) of the protonated **14** and mono-deprotonated **14**$_{-H}$ forms are indicated by the blue and green curves, respectively.

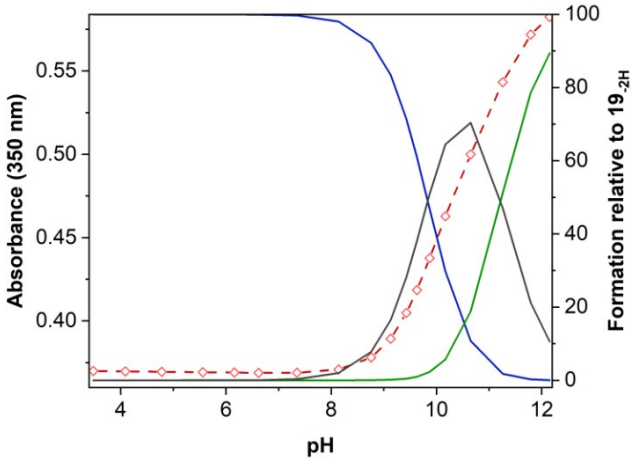

Figure S13. Hypspec2014 calculated concentration distribution curves for the equilibria species relative to the total complex concentration for **19**. The red diamonds indicate the experimental absorbance (350 nm) values, and the red dashed line represents the calculated curve for absorbance at 350 nm relative to solution pH. The solution speciation (concentrations) of the protonated **19**, mono-deprotonated **19**$_{-H}$ and di-deprotonated **19**$_{-2H}$ forms are indicated by the blue, black and green curves, respectively.

Table S2. Optimised geometry parameters of complex **13** in the ground state: percent error (δ) versus xc functionals with the LANL2DZ basis set and experimental data of **13**.

	Expt.	**B3LYP**		**M062X**		**mPW1PW91**	
item	**13**	**cal.**	**δ**	**cal.**	**δ**	**cal.**	**δ**
Bond Length, Å							
Ir-N1	2.047	2.07173	1.21	2.06543	0.90	2.05123	0.21
Ir-N2	2.047	2.07318	1.28	2.06347	0.80	2.04976	0.13
Ir-N3	2.175	2.20250	1.26	2.22020	2.08	2.16388	0.51
Ir-N4	2.144	2.17550	1.47	2.17969	1.66	2.13929	0.22
Ir-C1	2.016	2.02993	0.69	1.99760	0.91	2.01413	0.09
Ir-C2	2.020	2.02848	0.42	2.00076	0.95	2.01547	0.22
Total **δ**			6.33		7.30		1.38

Table S3. Optimised geometry parameters of complex **13** in the ground state: percent error (δ) versus xc functionals with the def2-SVP basis set and experimental data of **13**.

	Expt.	**B3LYP**		**M062X**		**mPW1PW91**	
item	**13**	**cal.**	**δ**	**cal.**	**δ**	**cal.**	**δ**
Bond Length, Å							
Ir-N1	2.047	2.08865	2.03	2.07939	1.58	2.06487	0.87
Ir-N2	2.047	2.08722	1.96	2.07681	1.46	2.06324	0.79
Ir-N3	2.175	2.26592	4.18	2.29659	5.59	2.22275	2.20
Ir-N4	2.144	2.23620	4.30	2.24925	4.91	2.19511	2.38
Ir-C1	2.016	2.02342	0.37	1.98164	1.70	2.00674	0.46
Ir-C2	2.020	2.02392	0.19	1.98471	1.75	2.00725	0.63
Total **δ**			13.03		16.99		7.33

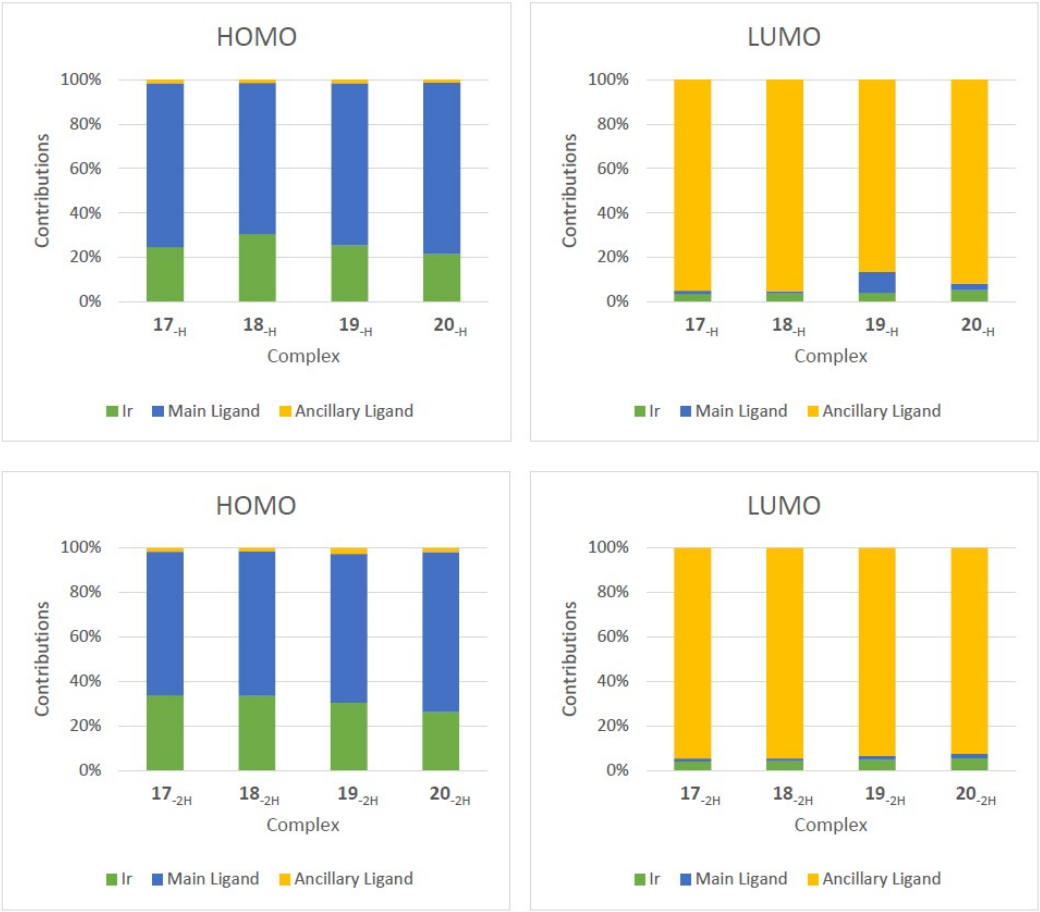

Figure S14. Calculated Mulliken populations of the frontier molecular orbitals (mPW1PW91/LANL2DZ level of theory) for the mono-deprotonated (**17**$_{-H}$ – **20**$_{-H}$) and di-deprotonated (**17**$_{-2H}$ – **20**$_{-2H}$) forms of complexes **17** – **20**.

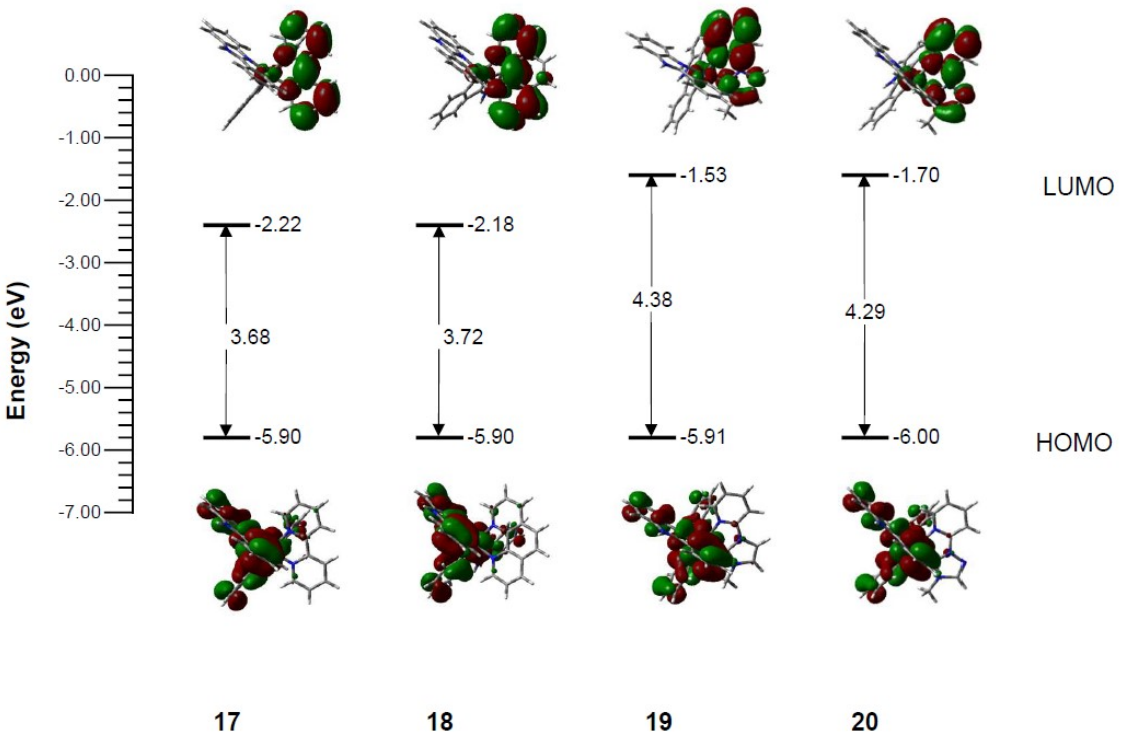

Figure S15. Contour plots of the HOMO and the LUMO orbitals in addition to the HOMO – LUMO energy band gaps for the protonated forms of complexes **17** – **20**. Isovalue = 0.02.

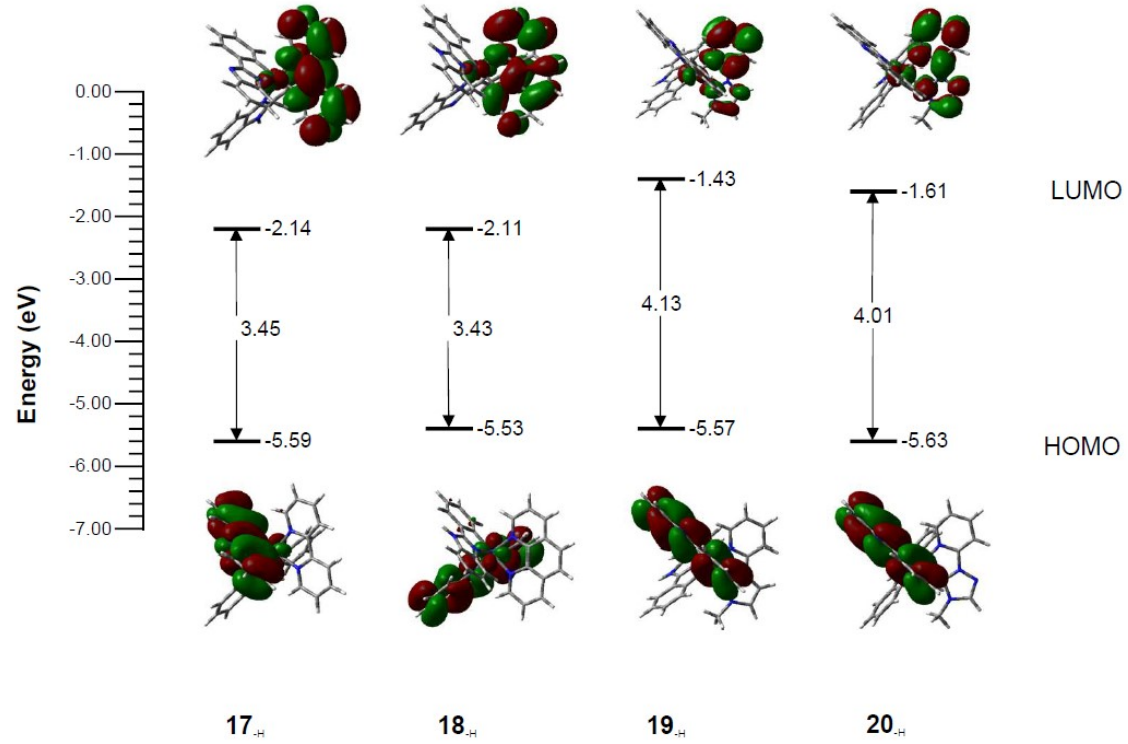

Figure S16. Contour plots of the HOMO and the LUMO orbitals in addition to the HOMO – LUMO energy band gaps for the deprotonated forms of complexes $\mathbf{17}_{-H}$ – $\mathbf{20}_{-H}$. Isovalue = 0.02.

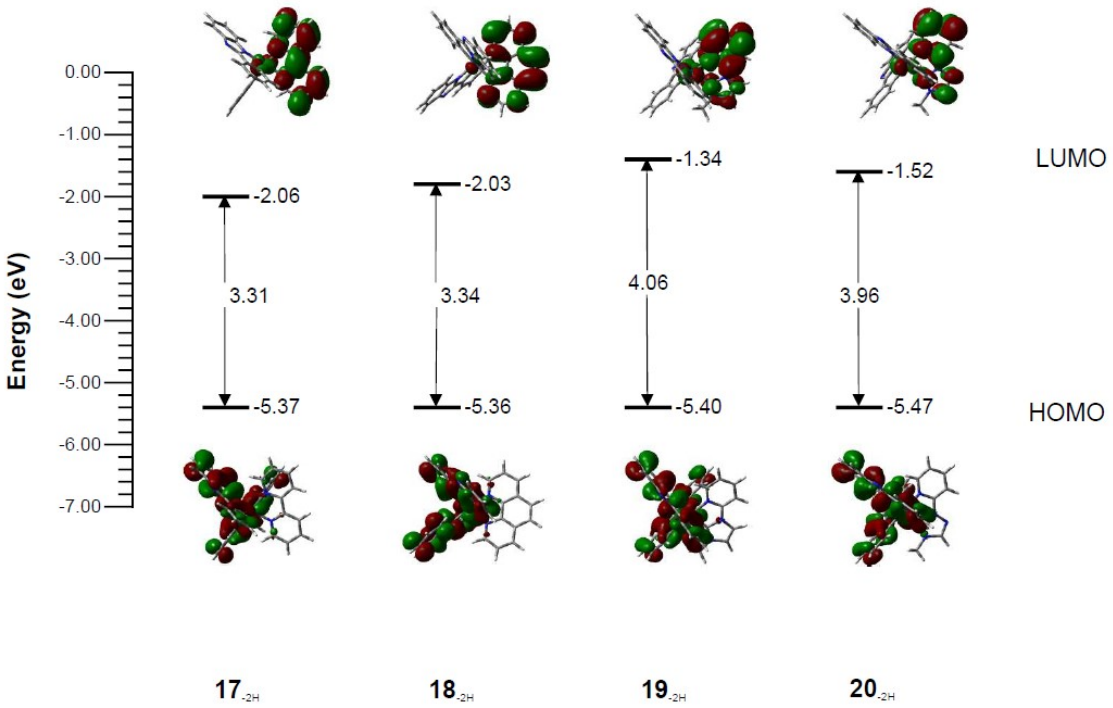

Figure S17. Contour plots of the HOMO and the LUMO orbitals in addition to the HOMO – LUMO energy band gaps for the di-deprotonated forms of complexes **17**$_{-2H}$ – **20**$_{-2H}$. Isovalue = 0.02.

Table S4. Phosphorescent emissions from TD-DFT calculations.

Complex	Emission (nm)	Major contributions
12 (protonated)	481	L→H (92%), L→H−1 (2%)
12 (deprotonated)	465	L→H (72%), L+1→H−2 (4%), L+1→H−3 (2%)
13 (protonated)	522	L→H (89%), L→H−1 (6%)
13 (deprotonated)	481	L→H−1 (58%), L→H (23%), L+1→H−1 (5%)
14 (protonated)	513	L→H (77%), L→H−1 (16%)
14 (deprotonated)	488	L→H (43%), L→H−1 (26%), L+1→H (10%), L+1→H−1 (6%)
15 (protonated)	548	L→H (95%)
15 (deprotonated)	473	L→H−1 (66%), L→H (21%)
16 (protonated)	573	L→H (96%)
16 (deprotonated)	443	L+1→H (41%), L→H (18%), L+1→H−2 (2%)
17 (protonated)	526	L→H (89%), L→H−4 (2%)
17 (semi-protonated)	589	L→H (76%), L→H−5 (4%)
17 (deprotonated)	642	L→H (88%)
18 (protonated)	520	L→H (77%), L→H−2 (4%), L→H−4 (2%)
18 (semi-protonated)	589	L→H (88%)
18 (deprotonated)	631	L→H (83%), L→H−2 (6%), L→H−6 (2%)
19 (protonated)	437	L+1→H (52%), L+1→H−1 (7%), L+2→H (7%) L+2→H−1 (4%), L+1→H−2 (3%)
19 (semi-protonated)	457	L→H (84%), L→H−3 (5%)
19 (deprotonated)	478	L→H (74%), L→H−1 (14%), L→H−4 (5%)
20 (protonated)	435	L+1→H (43%), L→H (14%), L→H−1 (5%), L+2→H (5%), L+1→H−2 (4%), L+3→H (4%), L+2→H−1 (3%), L+2→H−2 (2%)
20 (semi-protonated)	471	L→H (86%), L→H−2 (5%), L→H−3 (3%)
20 (deprotonated)	490	L→H (81%), L→H−1 (5%) L→H−4 (4%)

6. ^{1}H-NMR and ^{13}C-NMR Spectra

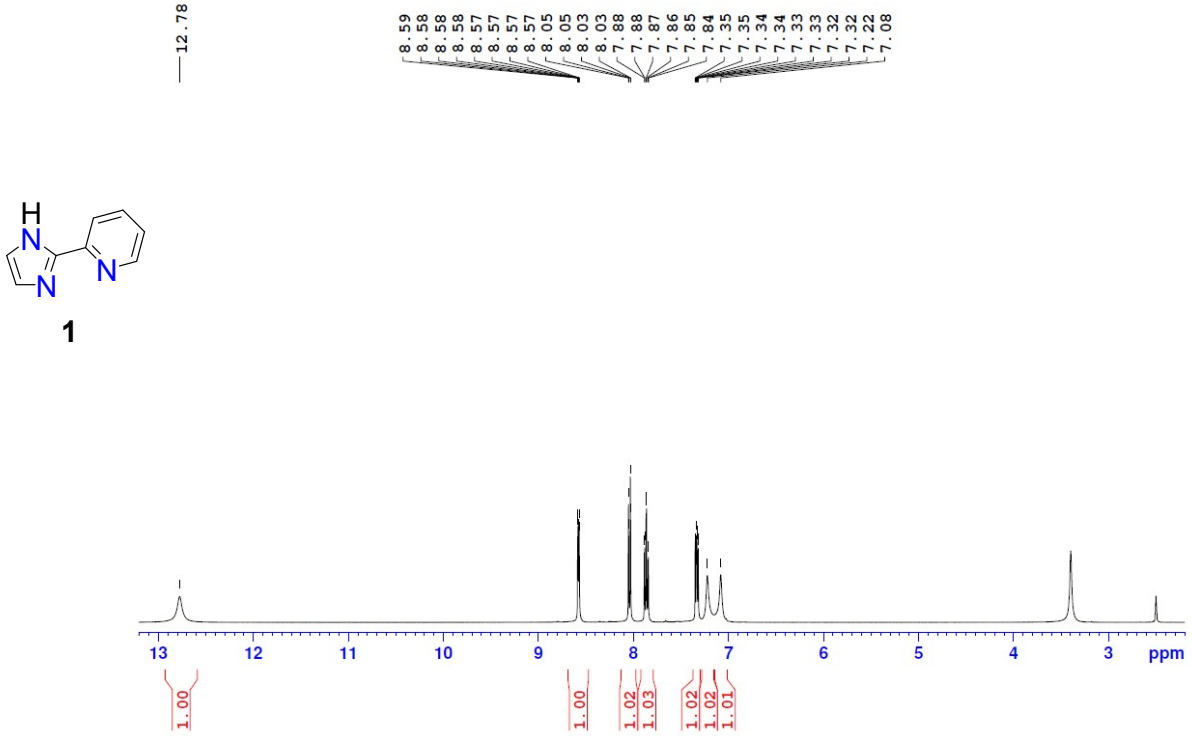

1

Figure S18. ^{1}H-NMR spectrum for **1** in DMSO.

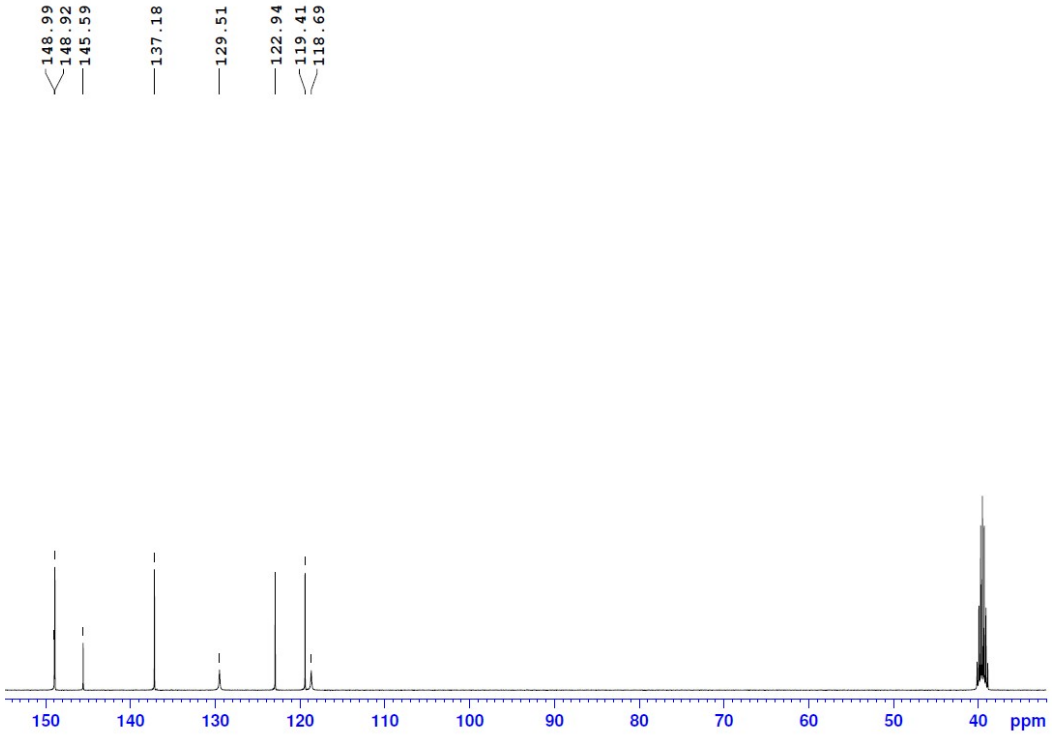

Figure S19. ^{13}C-NMR spectrum for **1** in DMSO.

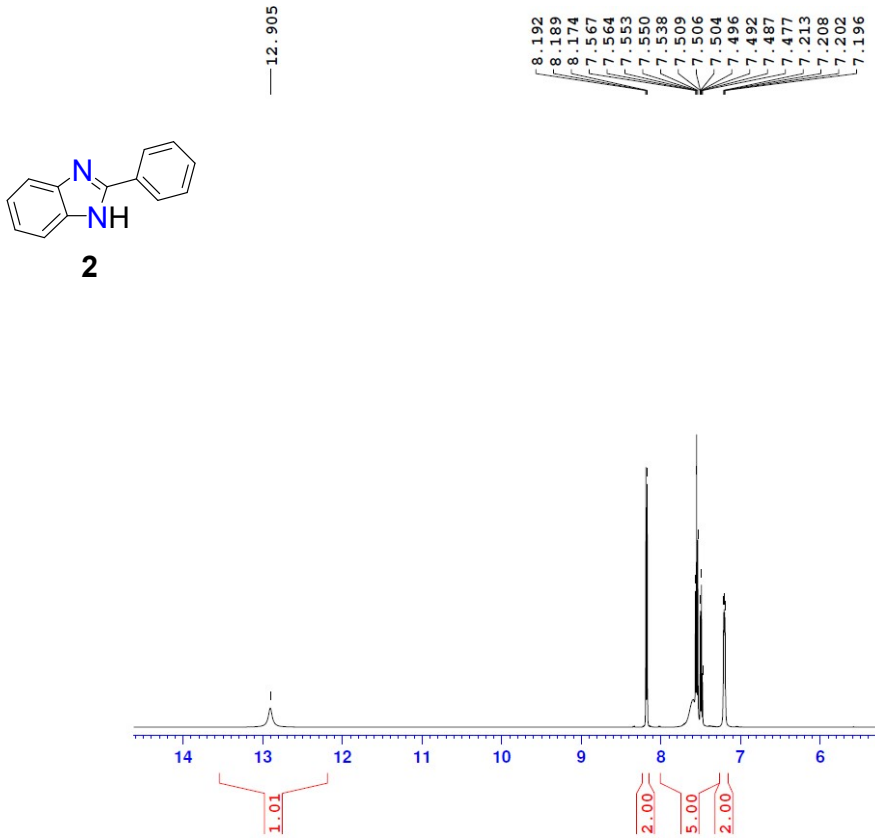

Figure S20. ^{1}H-NMR spectrum for **2** in DMSO.

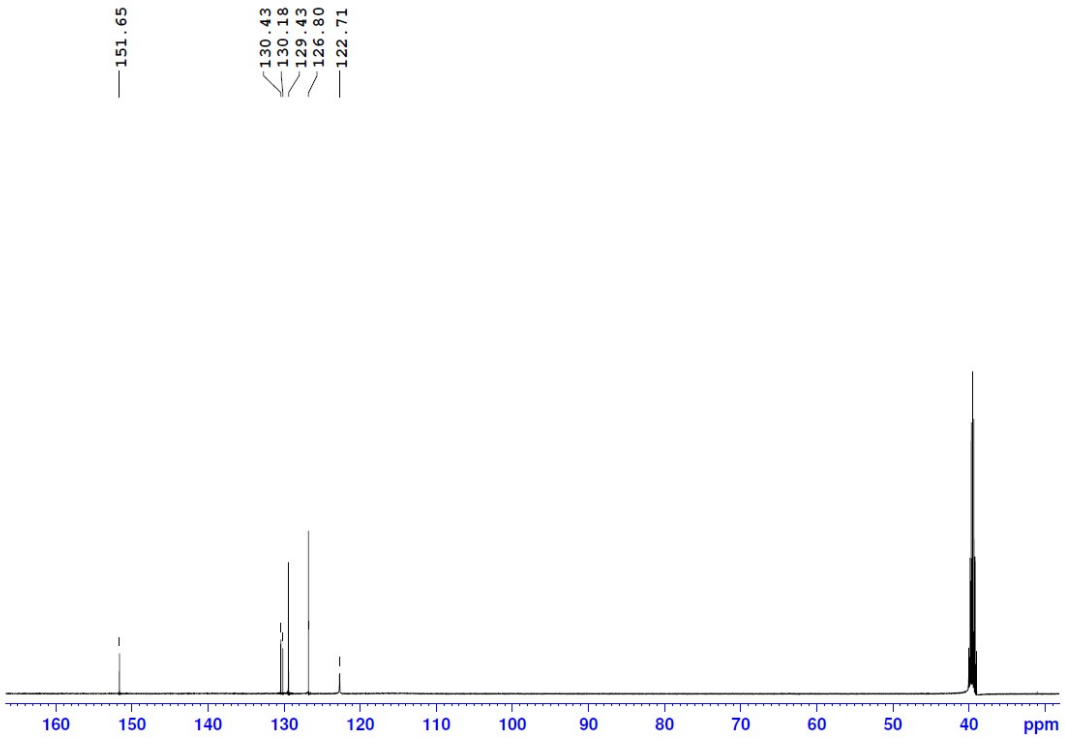

Figure S21. ^{13}C-NMR spectrum for **2** in DMSO.

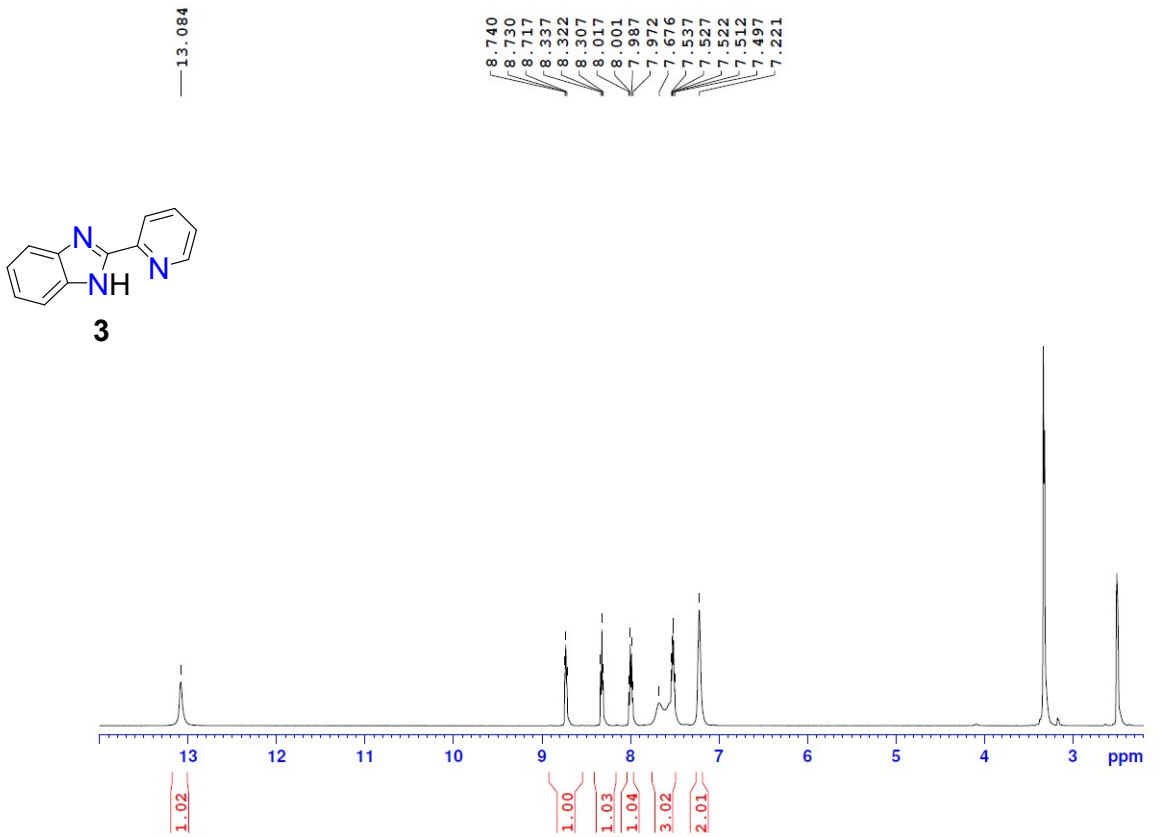

Figure S22. ^{1}H-NMR spectrum for **3** in DMSO.

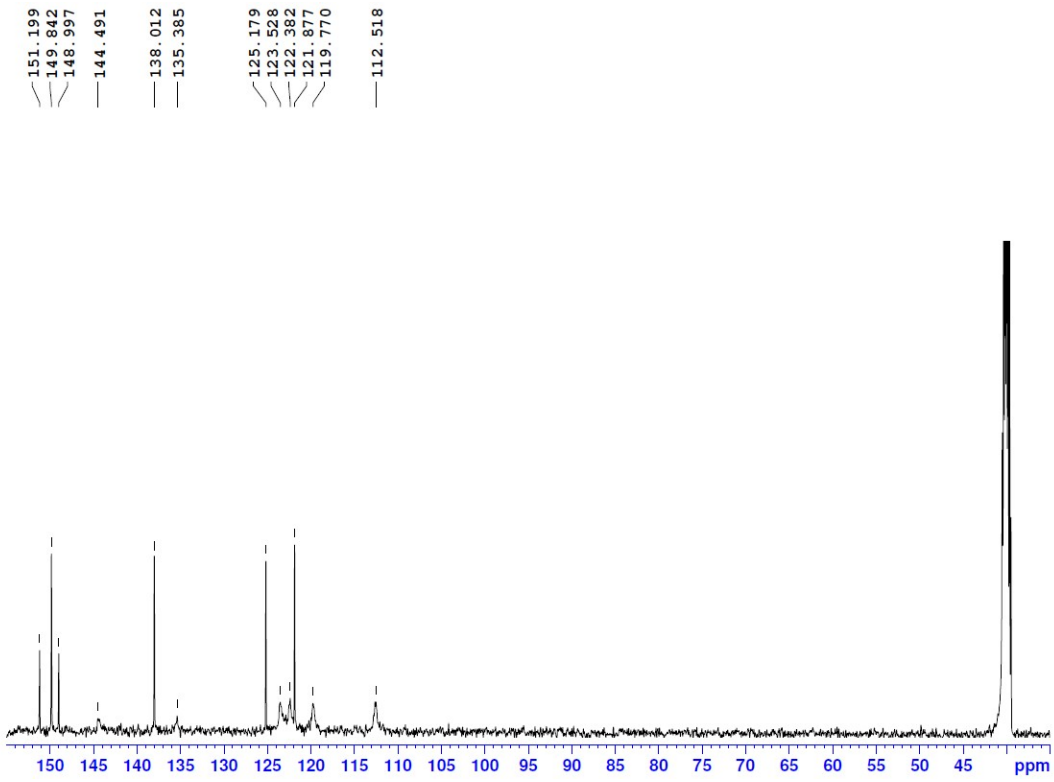

Figure S23. ^{13}C-NMR spectrum for **3** in DMSO.

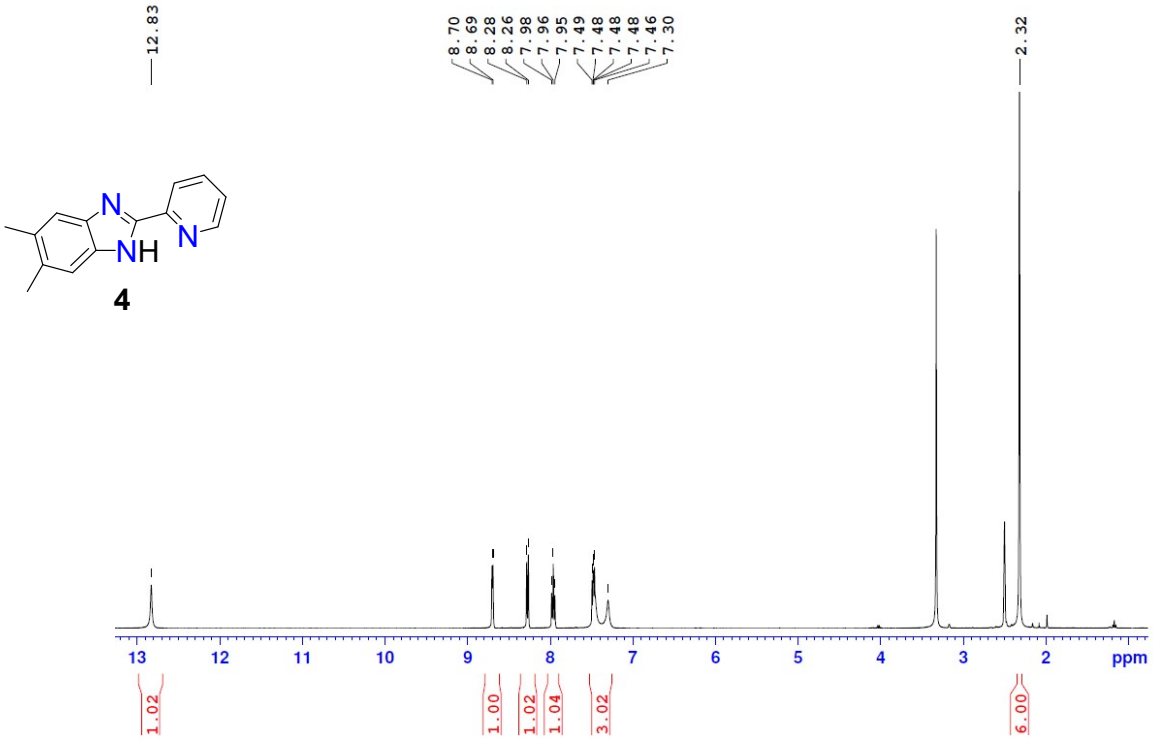

Figure S24. ^{1}H-NMR spectrum for **4** in DMSO.

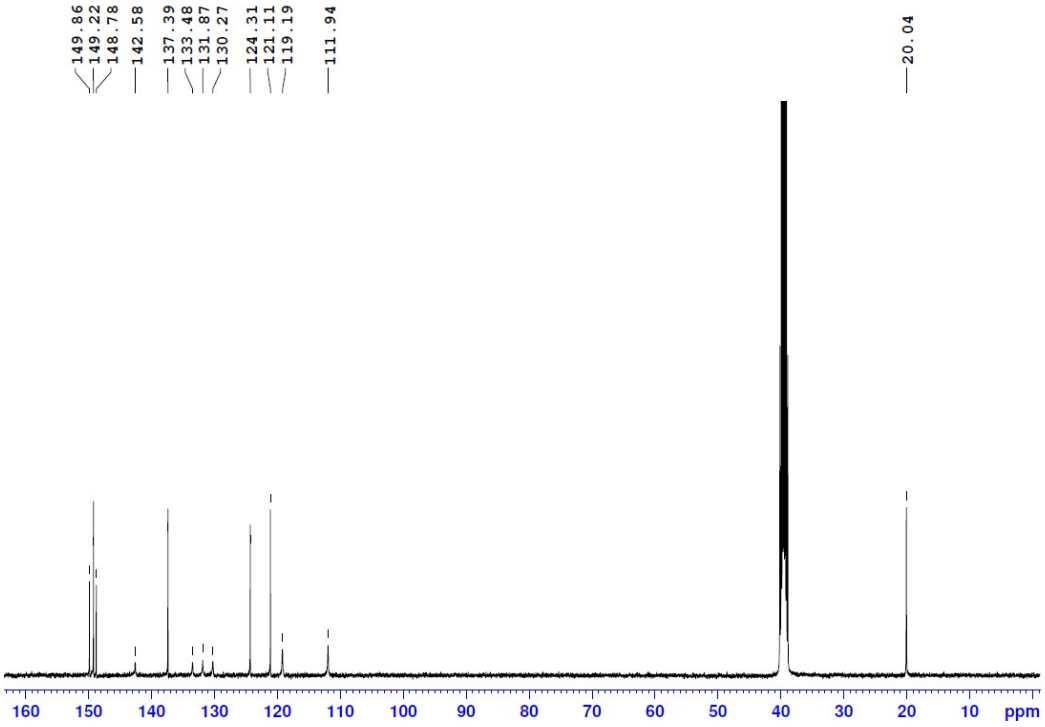

Figure S25. ^{13}C-NMR spectrum for **4** in DMSO.

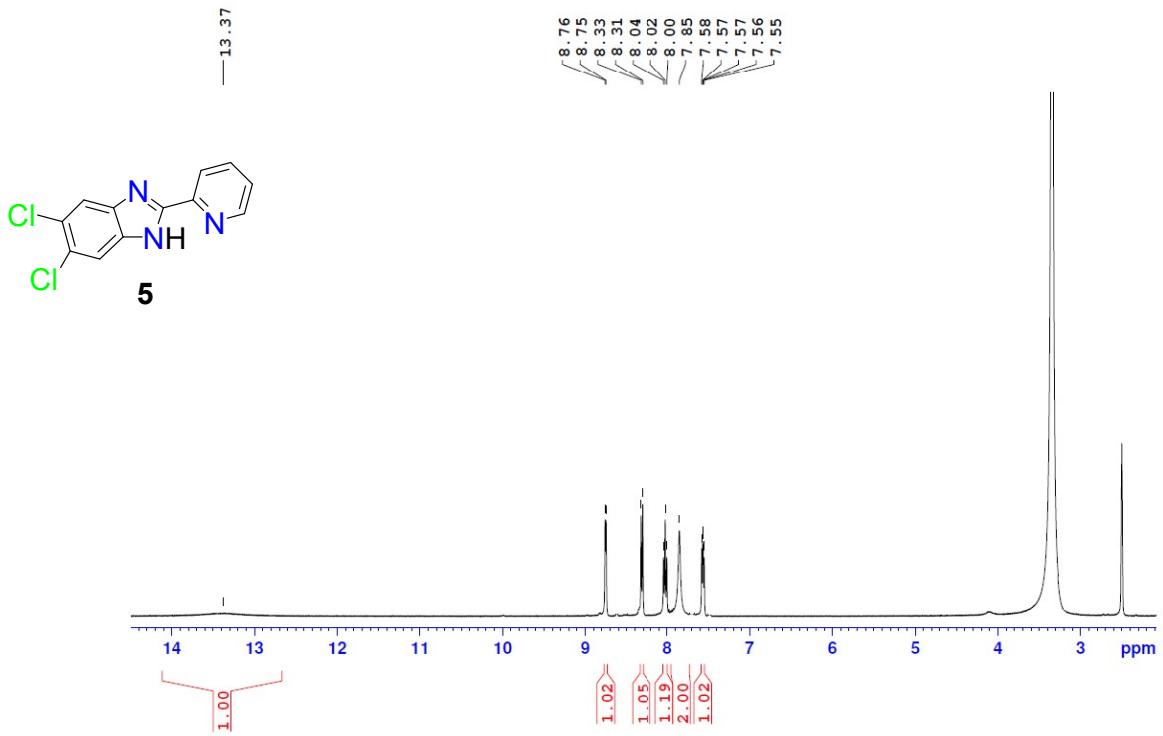

Figure S26. [1]H-NMR spectrum for **5** in DMSO.

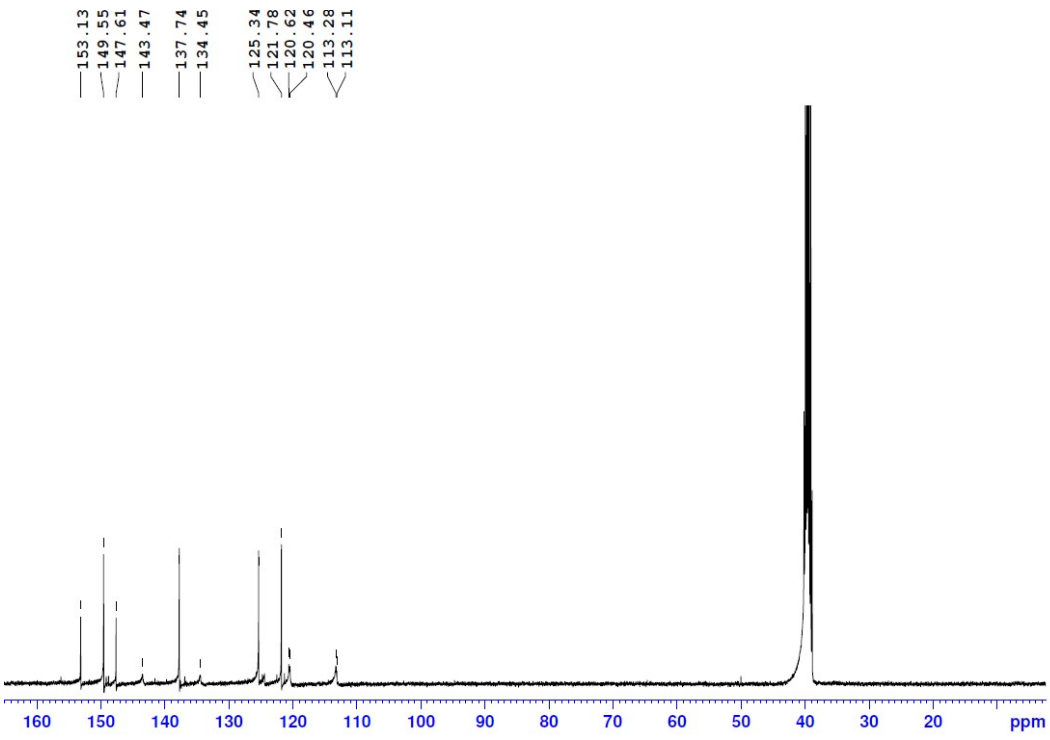

Figure S27. [13]C-NMR spectrum for **5** in DMSO.

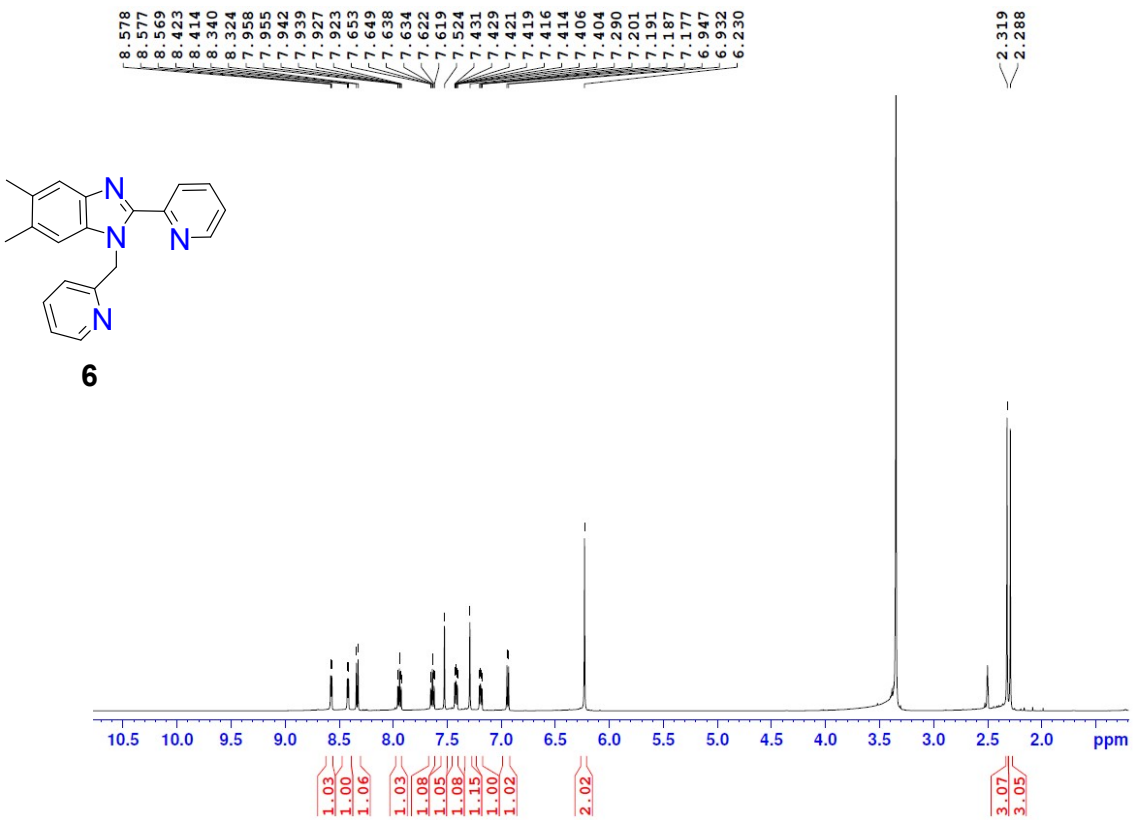

Figure S28. ^{1}H-NMR spectrum for **6** in DMSO.

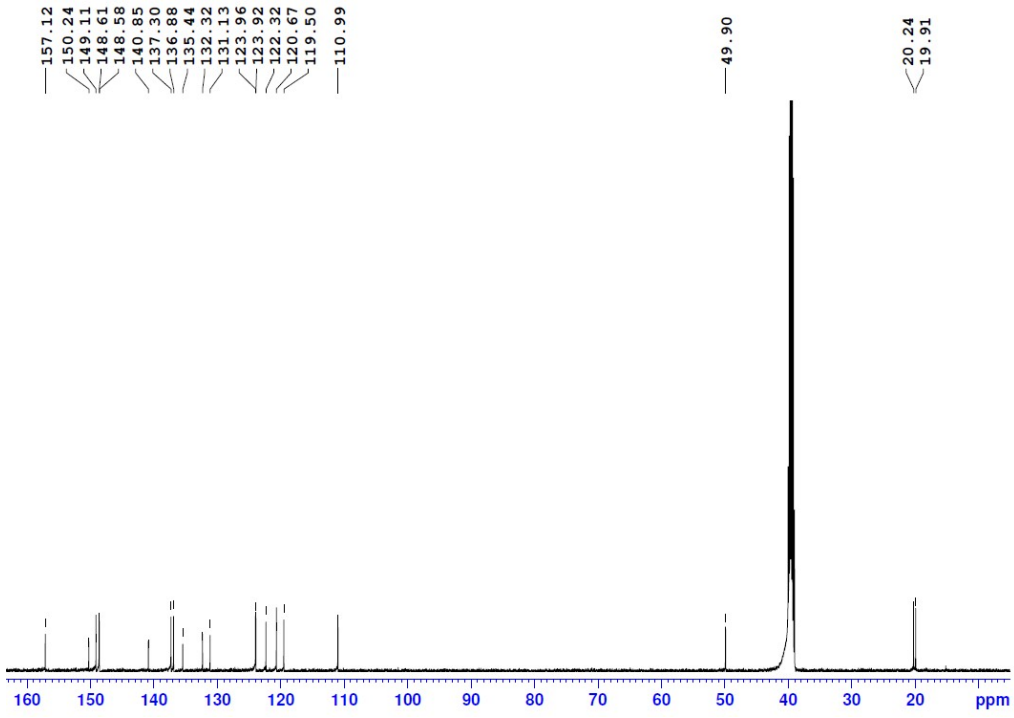

Figure S29. ^{13}C-NMR spectrum for **6** in DMSO.

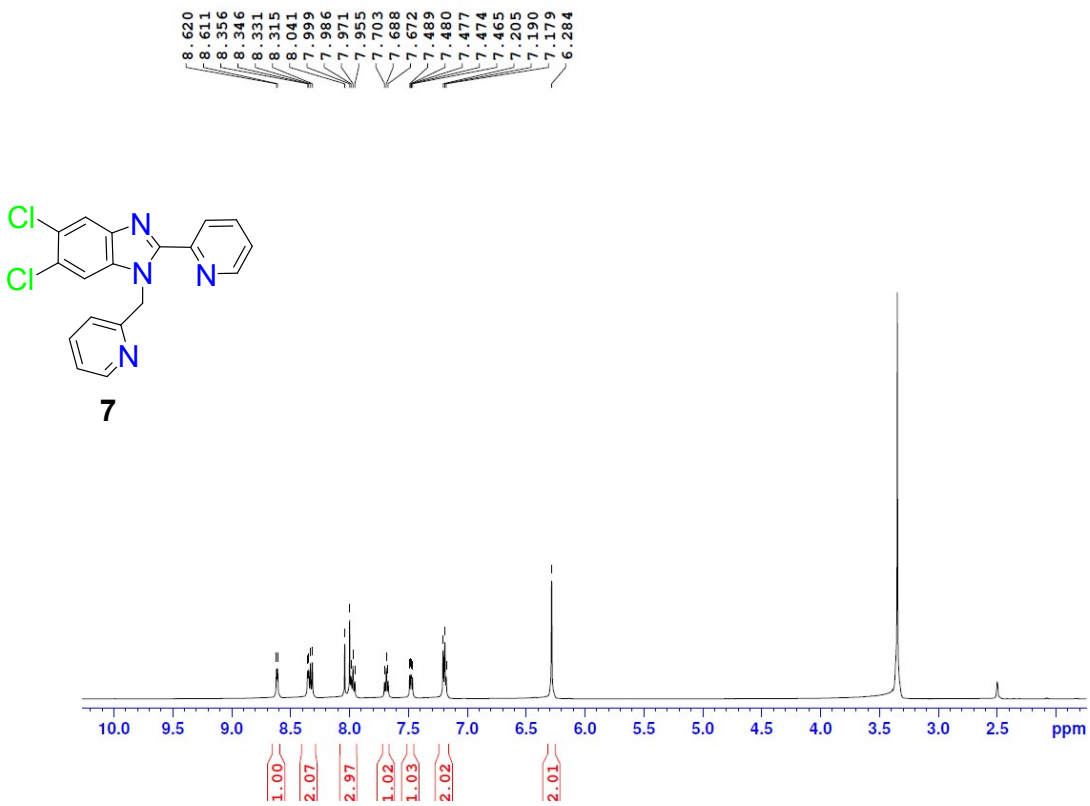

Figure S30. ^{1}H-NMR spectrum for **7** in DMSO.

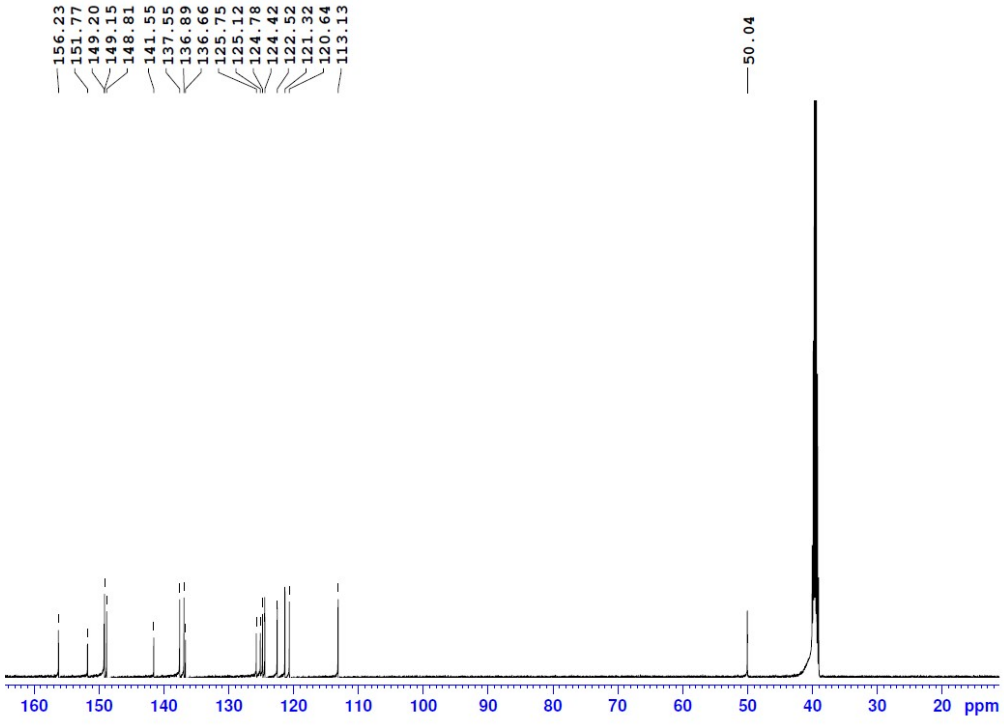

Figure S31. ^{13}C-NMR spectrum for **7** in DMSO.

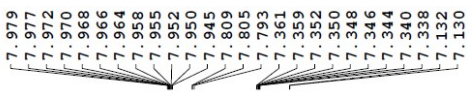

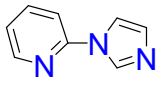

8

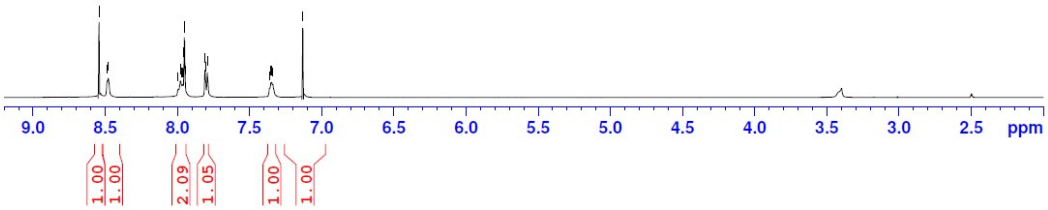

Figure S32. ^{1}H-NMR spectrum for **8** in DMSO.

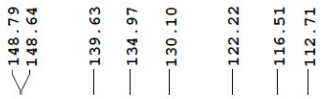

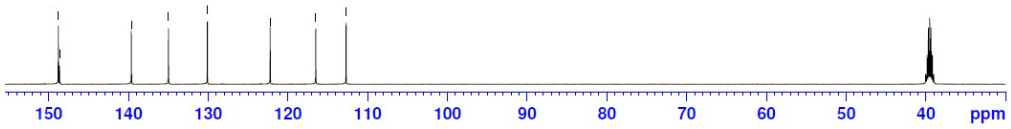

Figure S33. ^{13}C-NMR spectrum for **8** in DMSO.

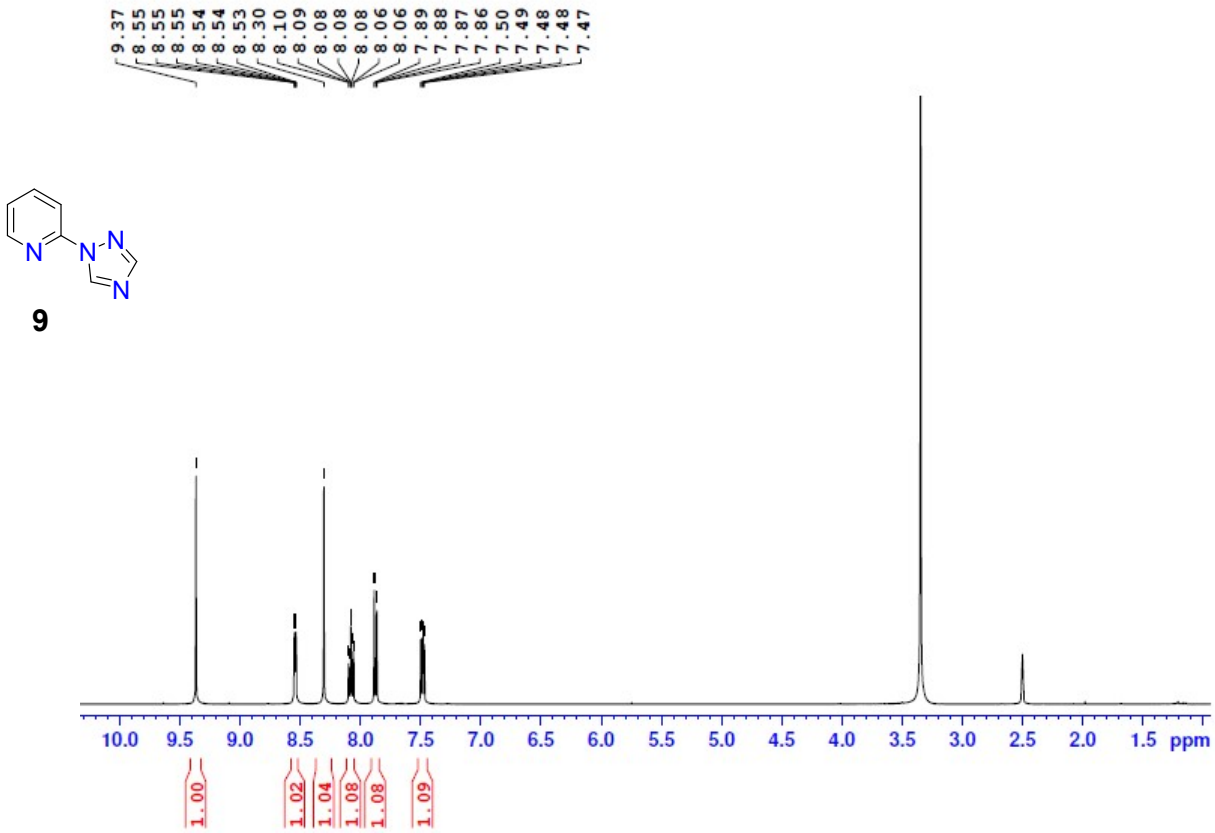

Figure S34. ^{1}H-NMR spectrum for **9** in DMSO.

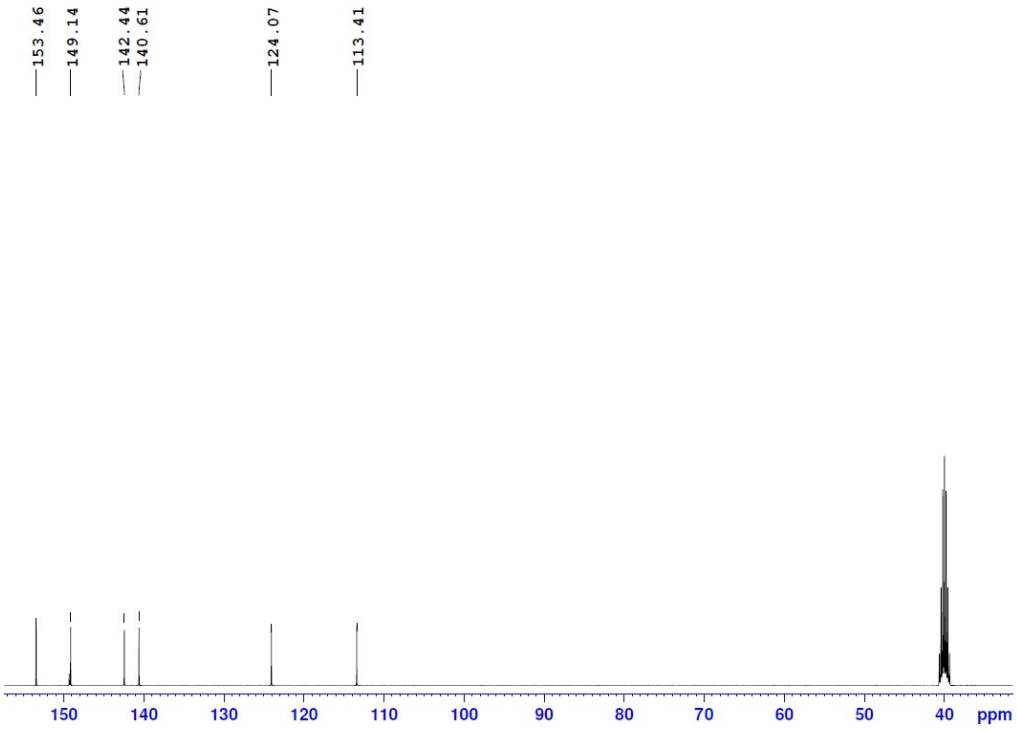

Figure S35. ^{13}C-NMR spectrum for **9** in DMSO.

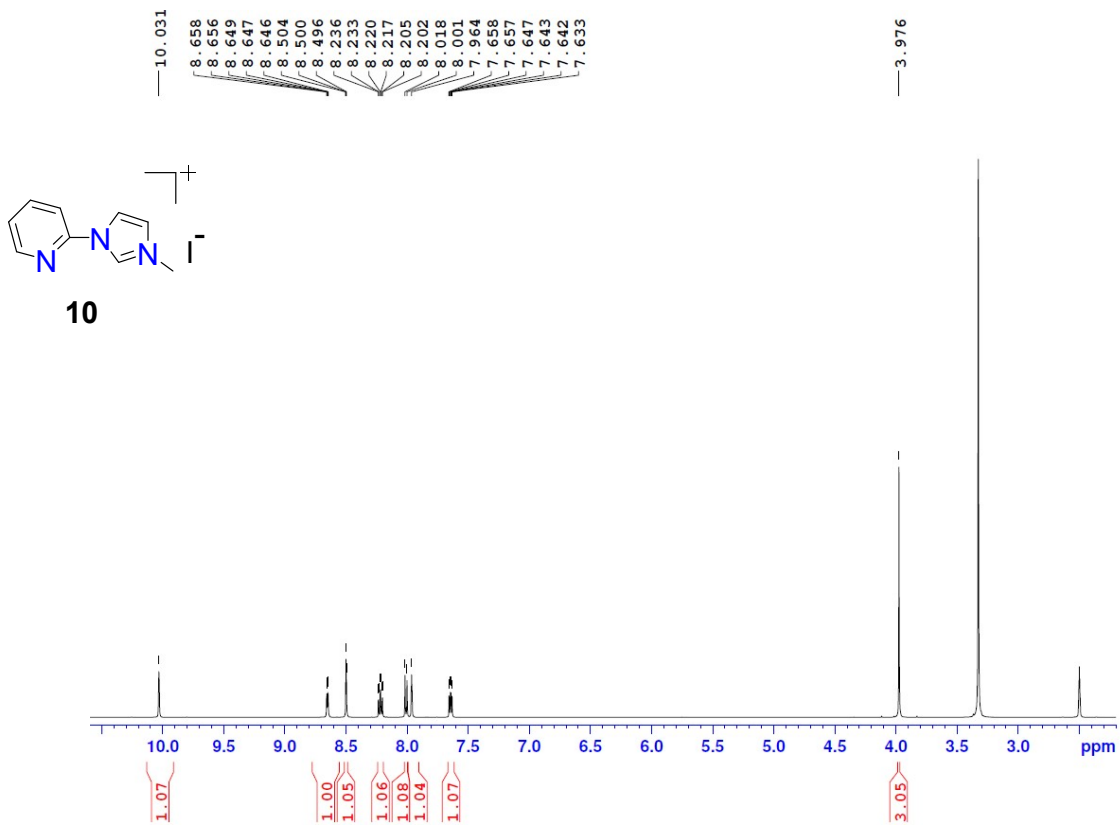

Figure S36. ^{1}H-NMR spectrum for **10** in DMSO.

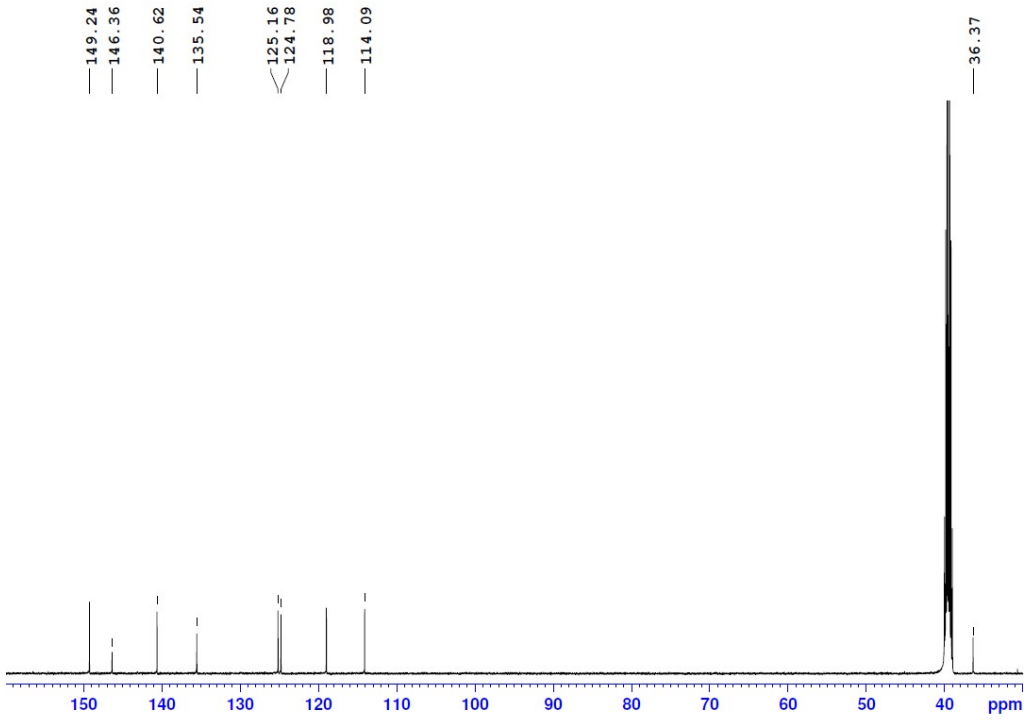

Figure S37. ^{13}C-NMR spectrum for **10** in DMSO.

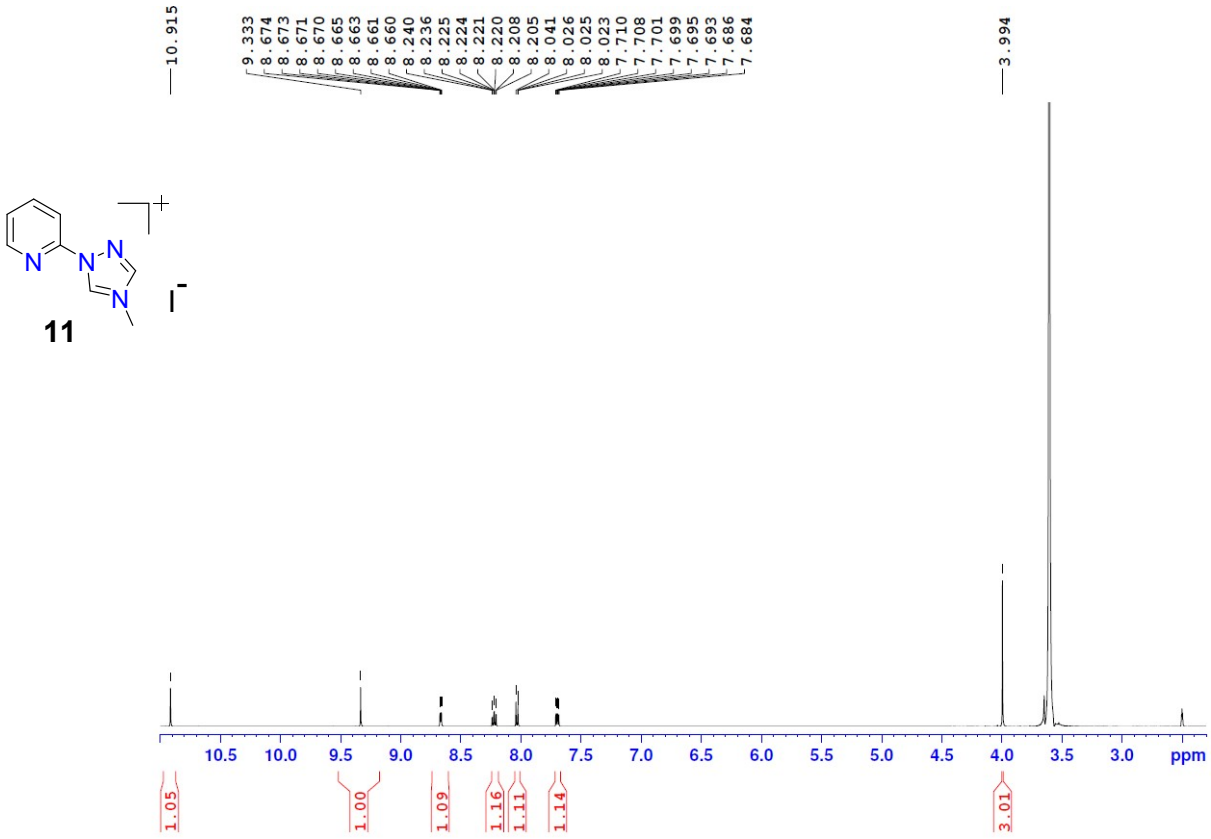

Figure S38. ^{1}H-NMR spectrum for **11** in DMSO.

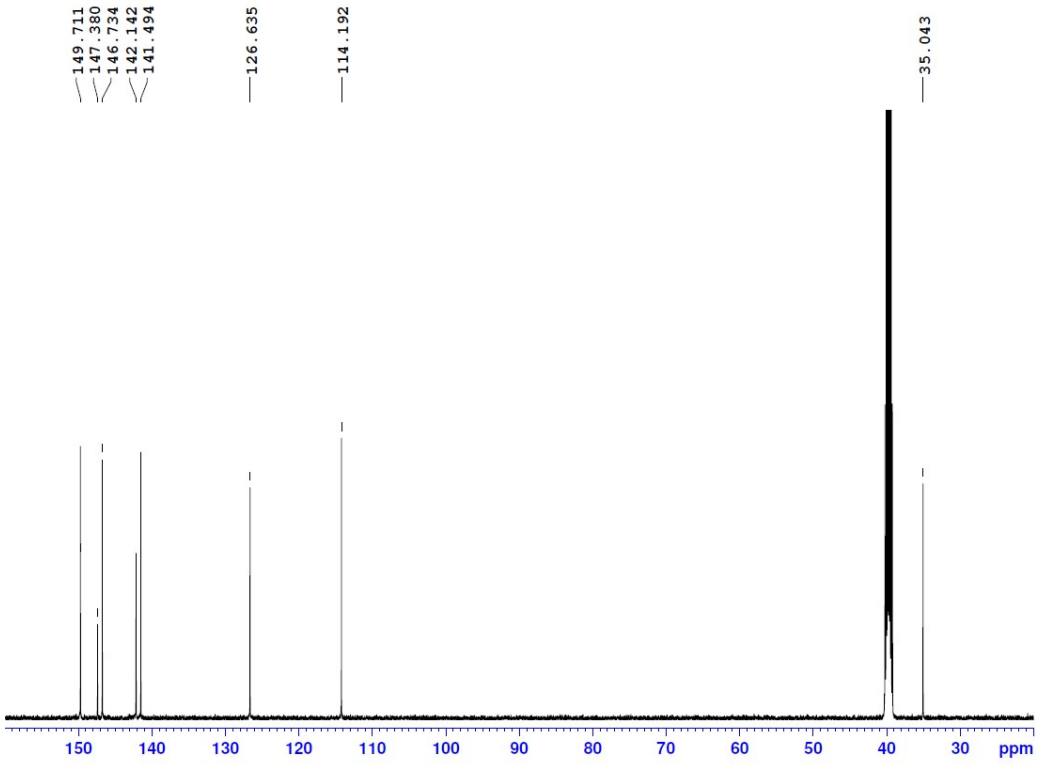

Figure S39. ^{13}C-NMR spectrum for **11** in DMSO.

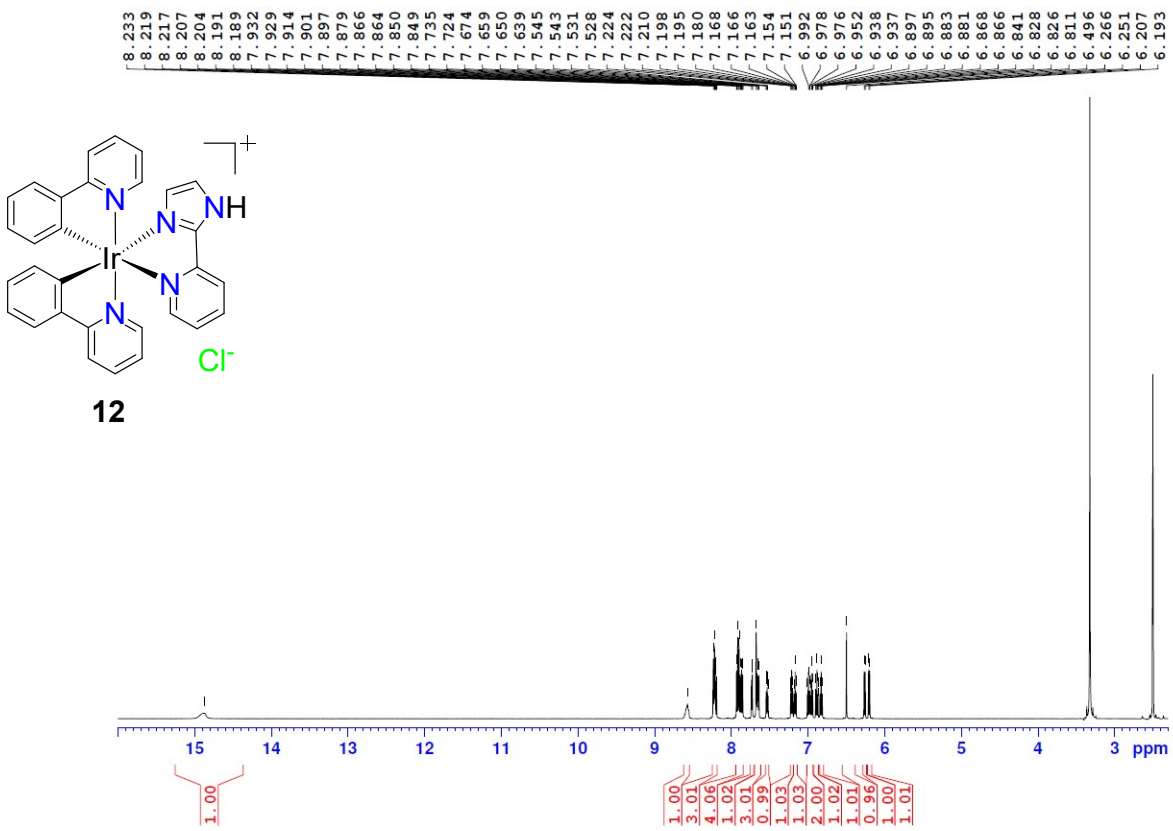

Figure S40. ^{1}H-NMR spectrum for **12** in DMSO.

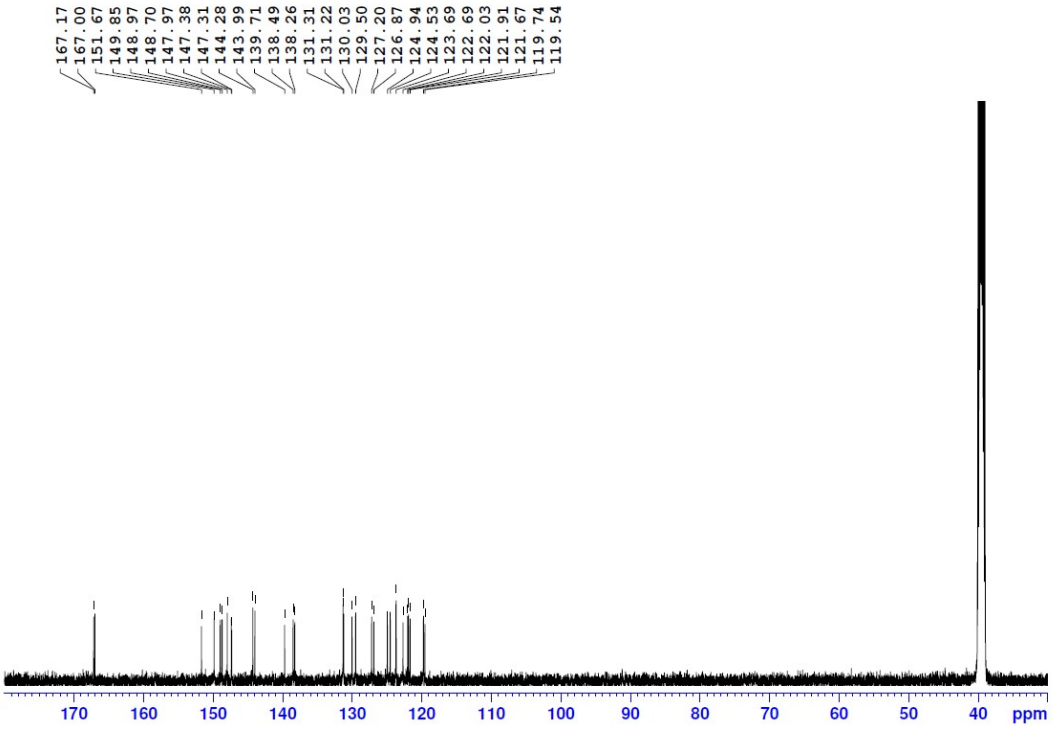

Figure S41. ^{13}C-NMR spectrum for **12** in DMSO.

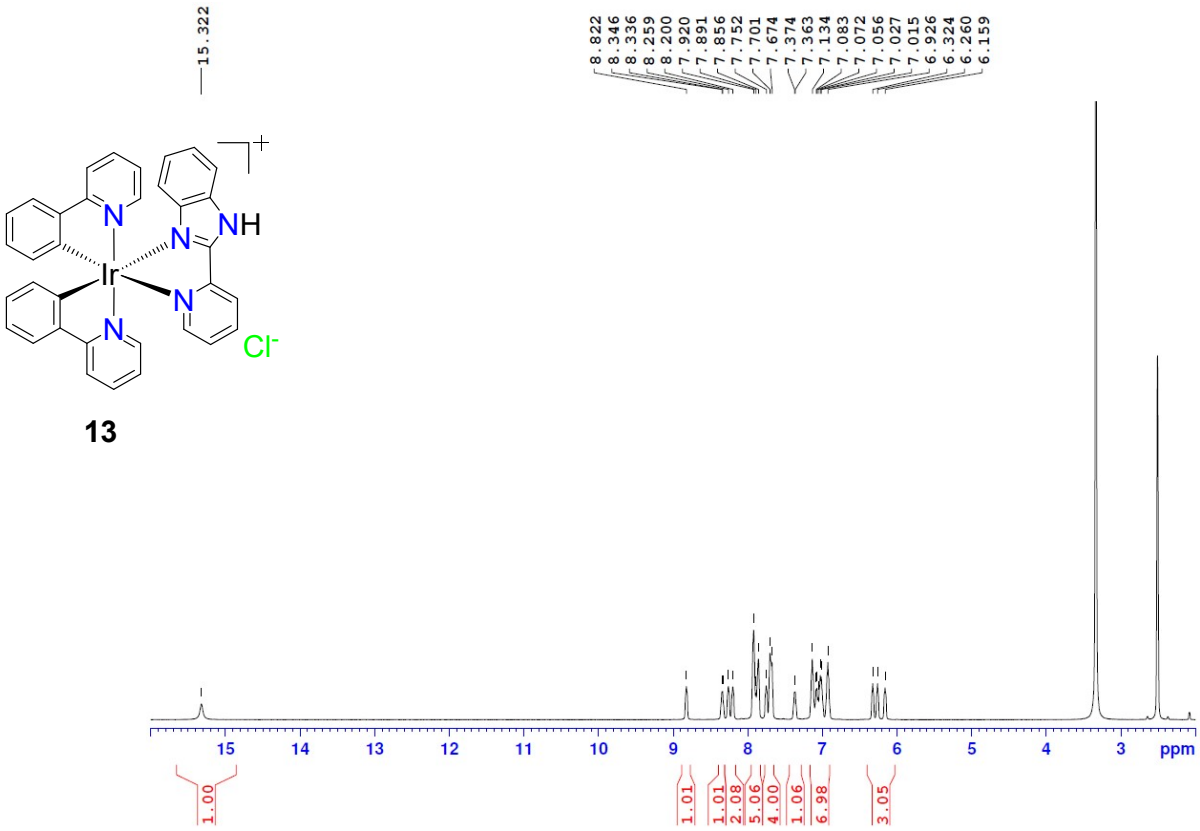

Figure S42. ^{1}H-NMR spectrum for **13** in DMSO.

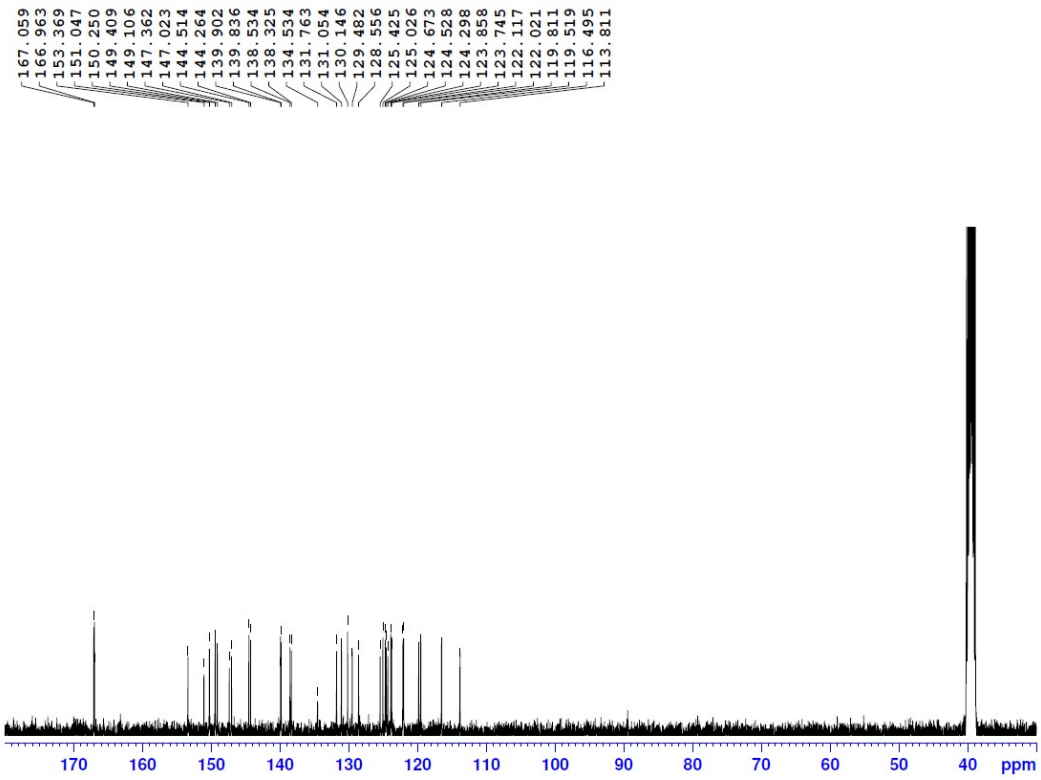

Figure S43. ^{13}C-NMR spectrum for **13** in DMSO.

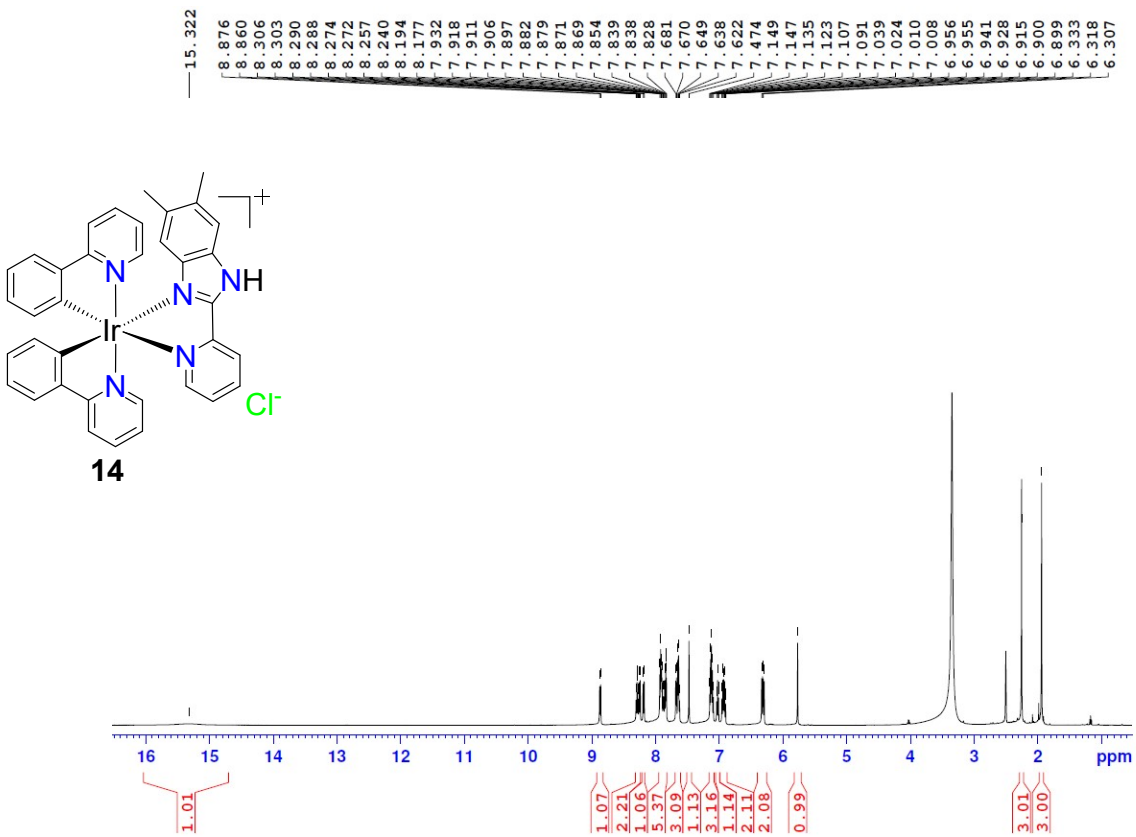

Figure S44. ^{1}H-NMR spectrum for **14** in DMSO.

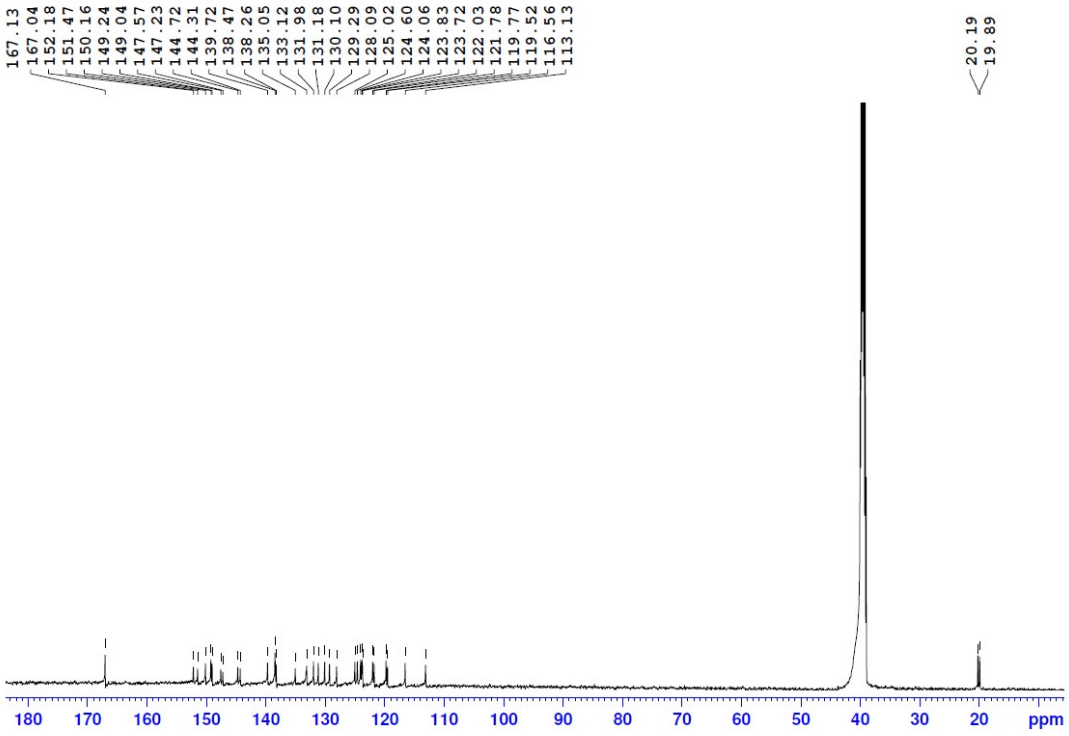

Figure S45. ^{13}C-NMR spectrum for **14** in DMSO.

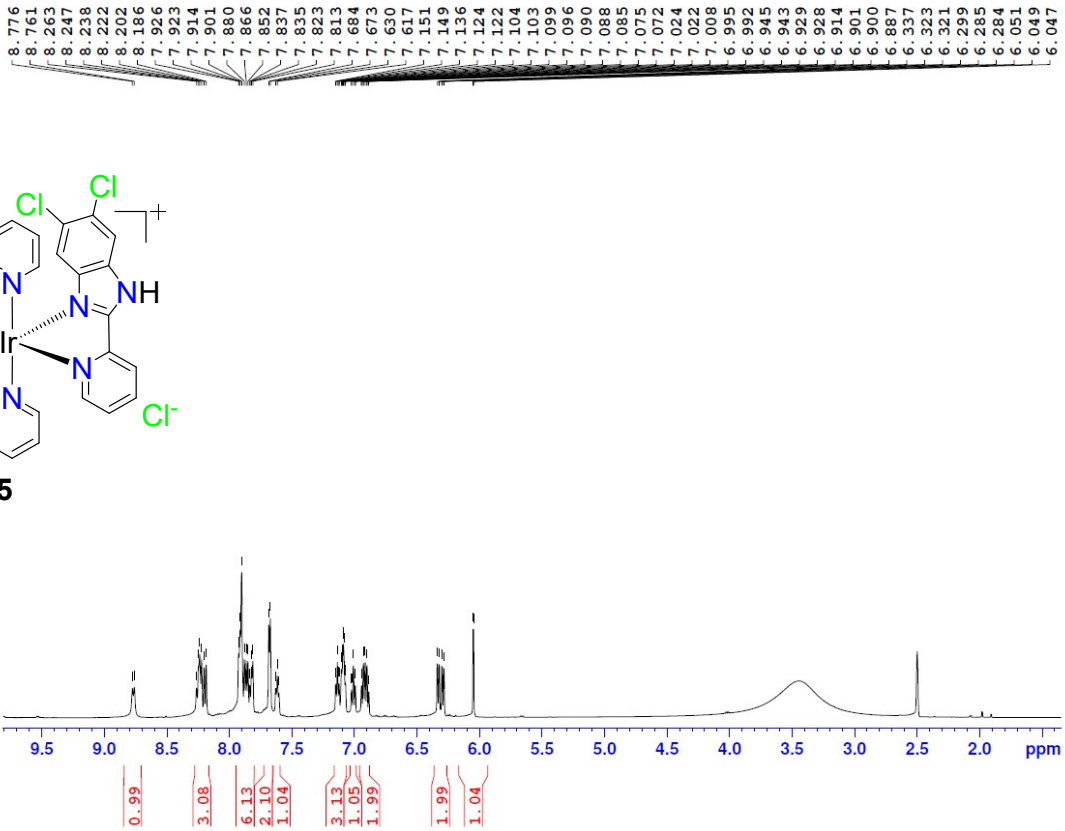

Figure S46. ^{1}H-NMR spectrum for **15** in DMSO.

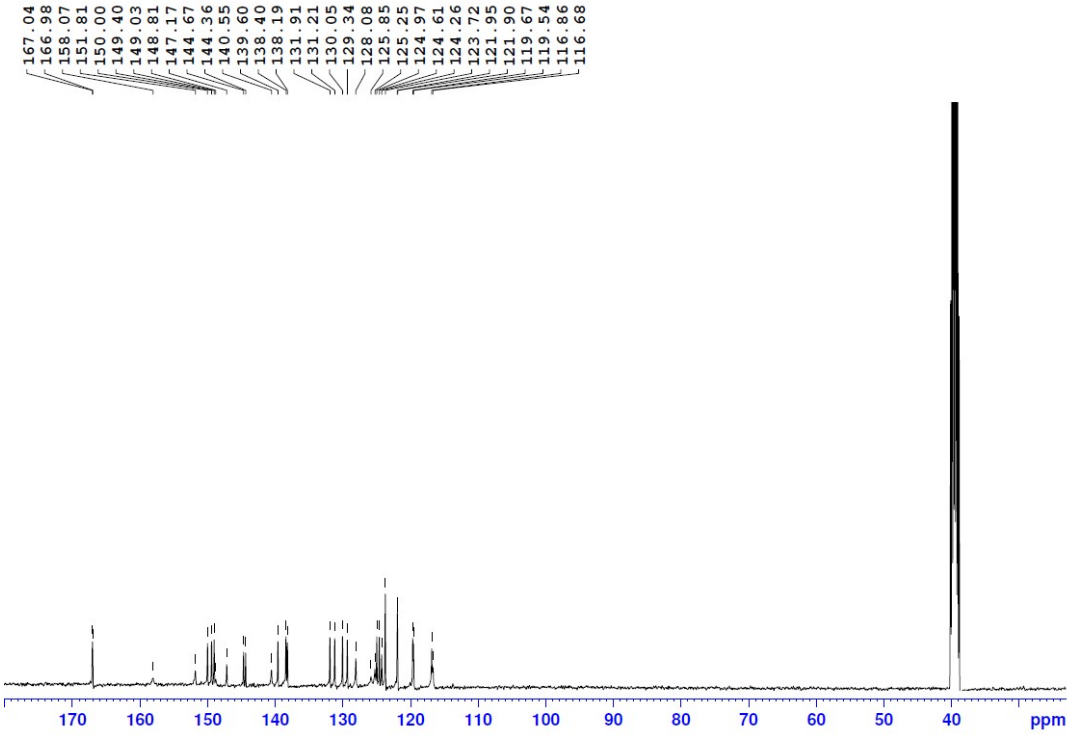

Figure S47. ^{13}C-NMR spectrum for **15** in DMSO.

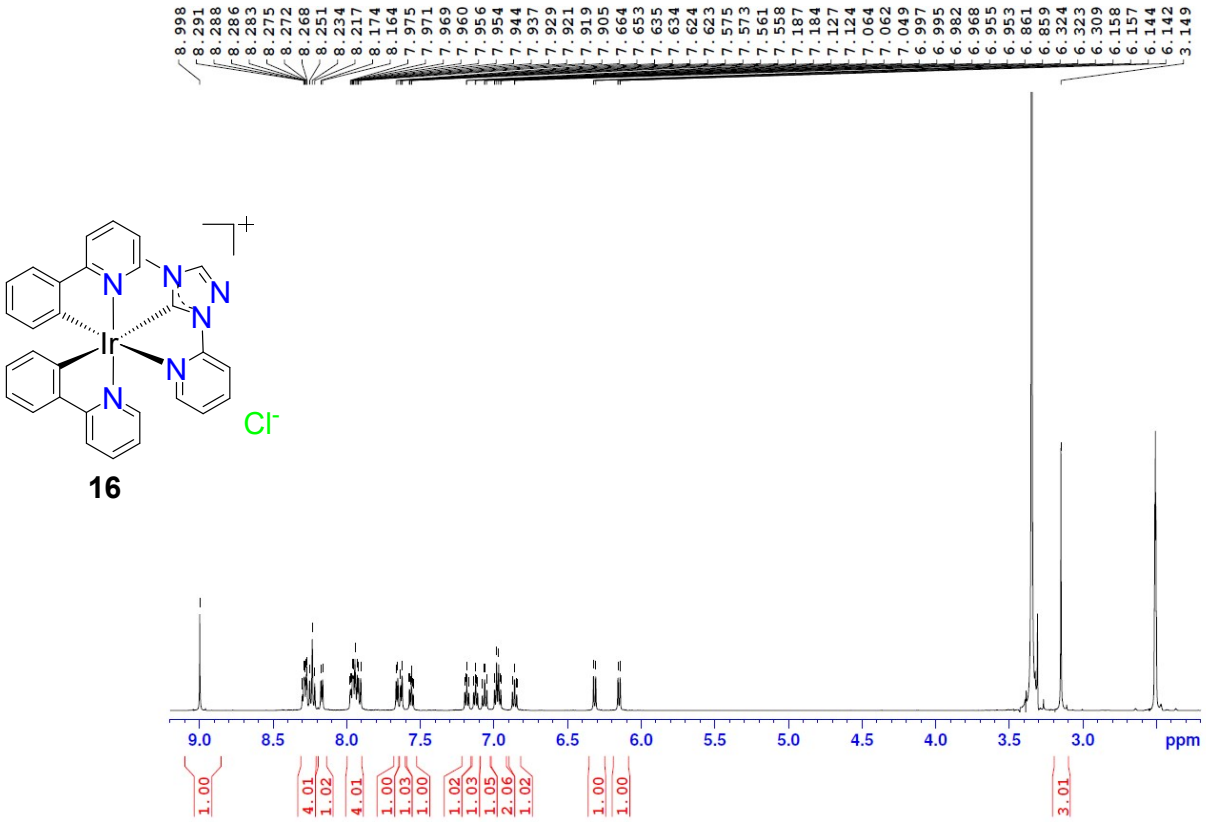

Figure S48. ^{1}H-NMR spectrum for **16** in DMSO.

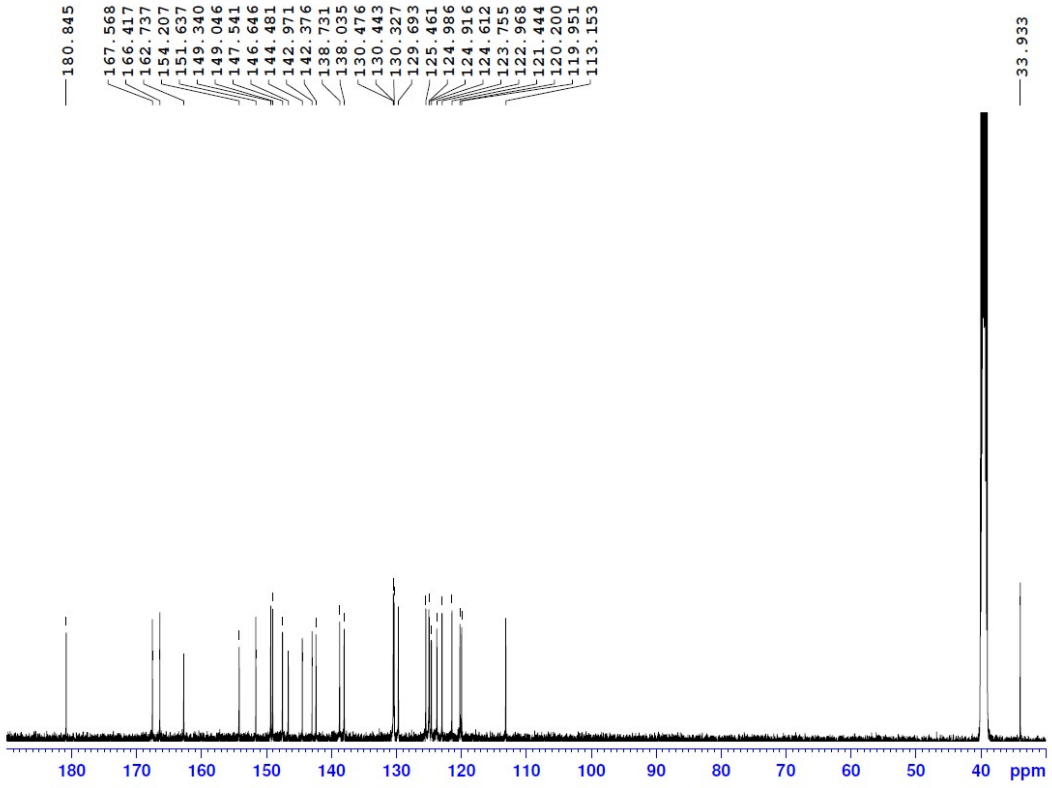

Figure S49. ^{13}C-NMR spectrum for **16** in DMSO.

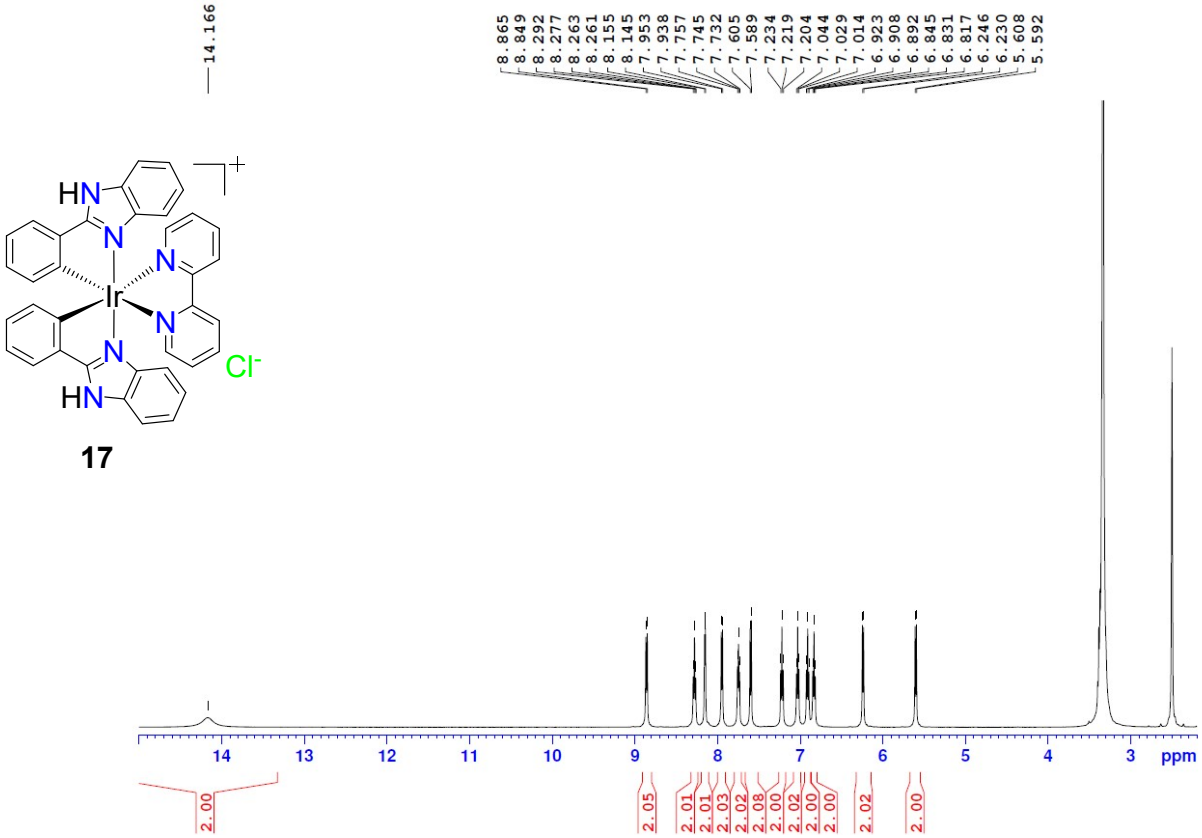

Figure S50. ^{1}H-NMR spectrum for **17** in DMSO.

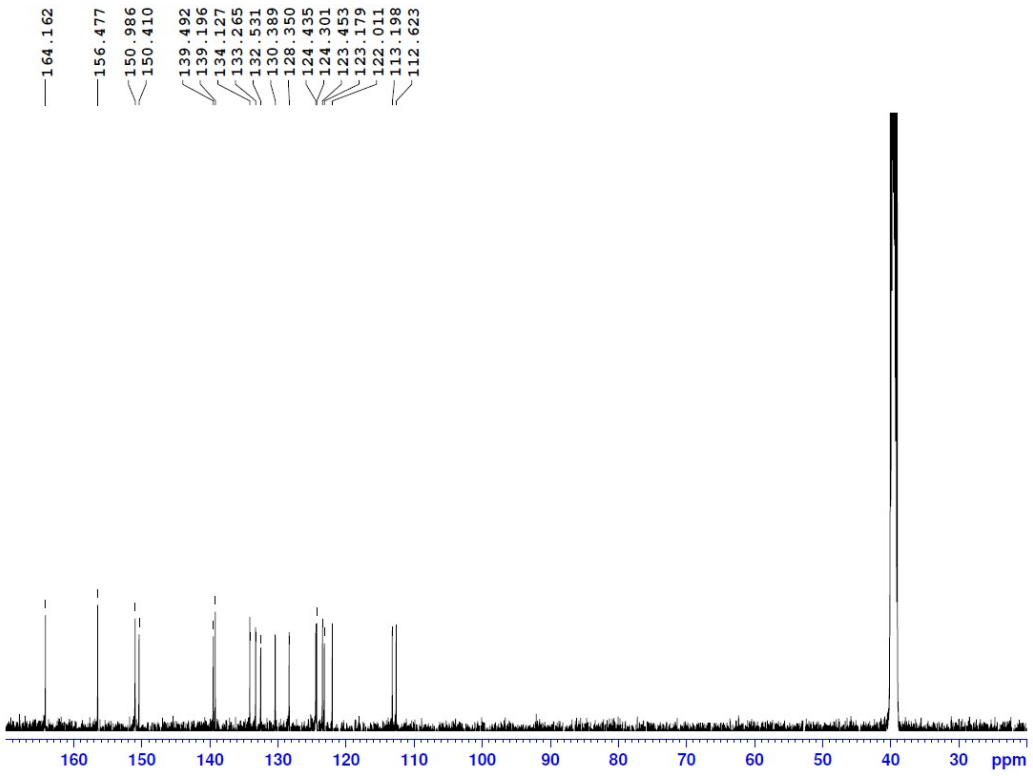

Figure S51. ^{13}C-NMR spectrum for **17** in DMSO.

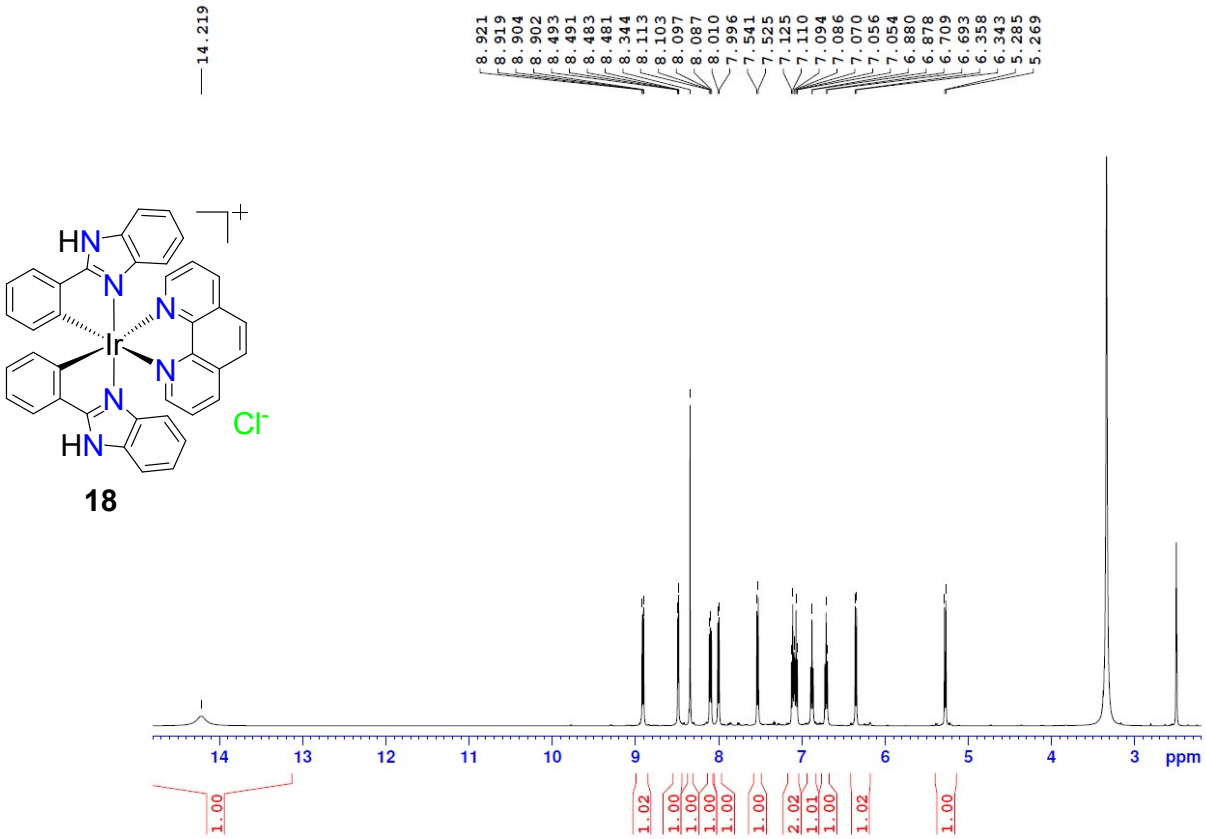

Figure S52. ^{1}H-NMR spectrum for **18** in DMSO.

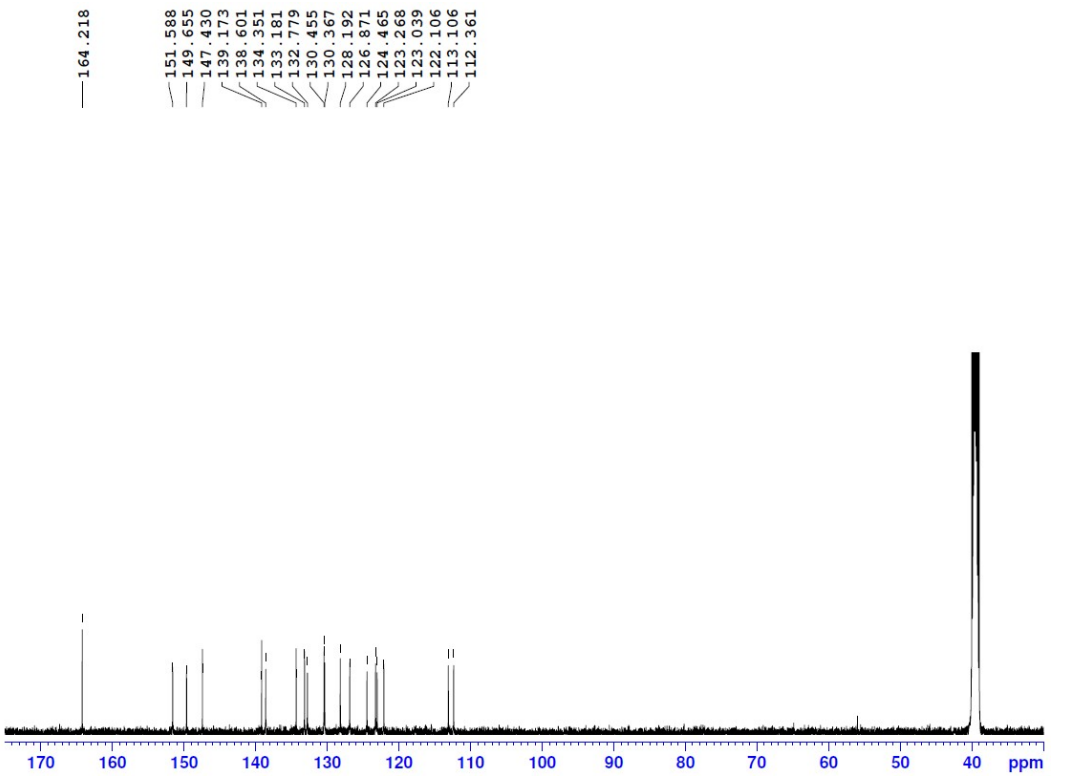

Figure S53. ^{13}C-NMR spectrum for **18** in DMSO.

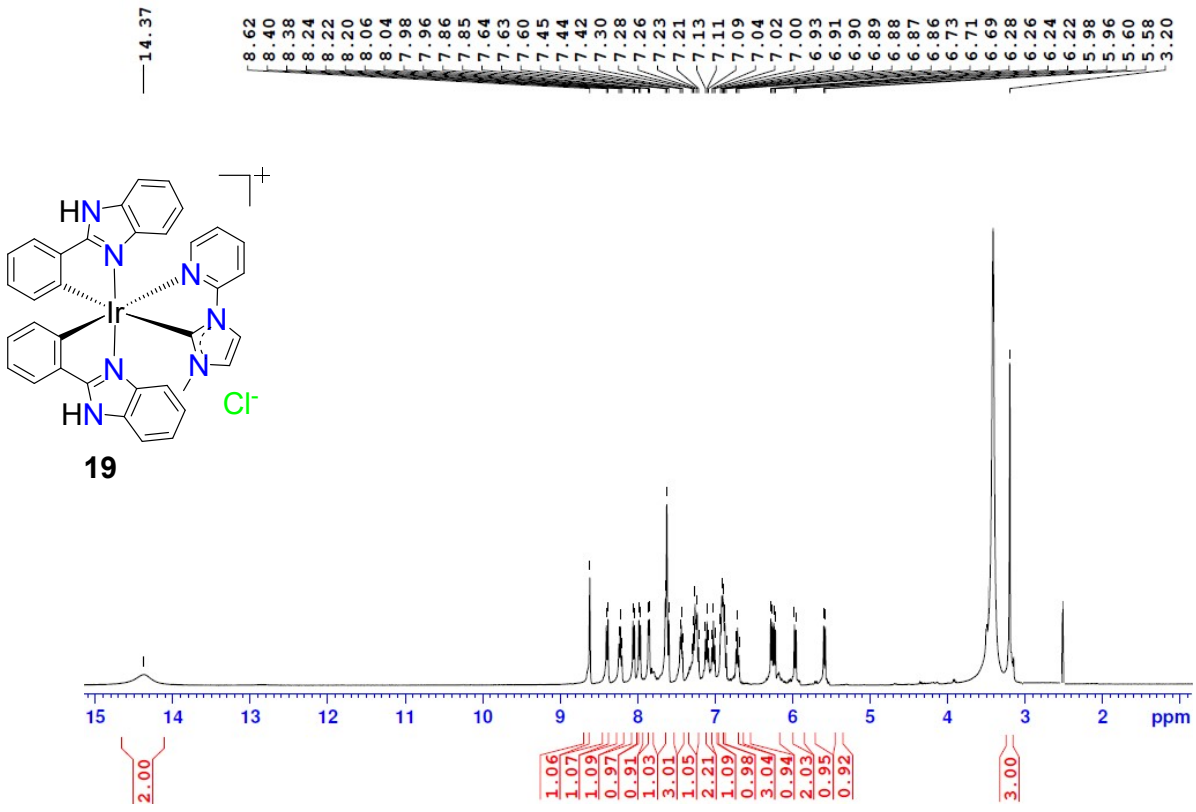

Figure S54. ^{1}H-NMR spectrum for **19** in DMSO.

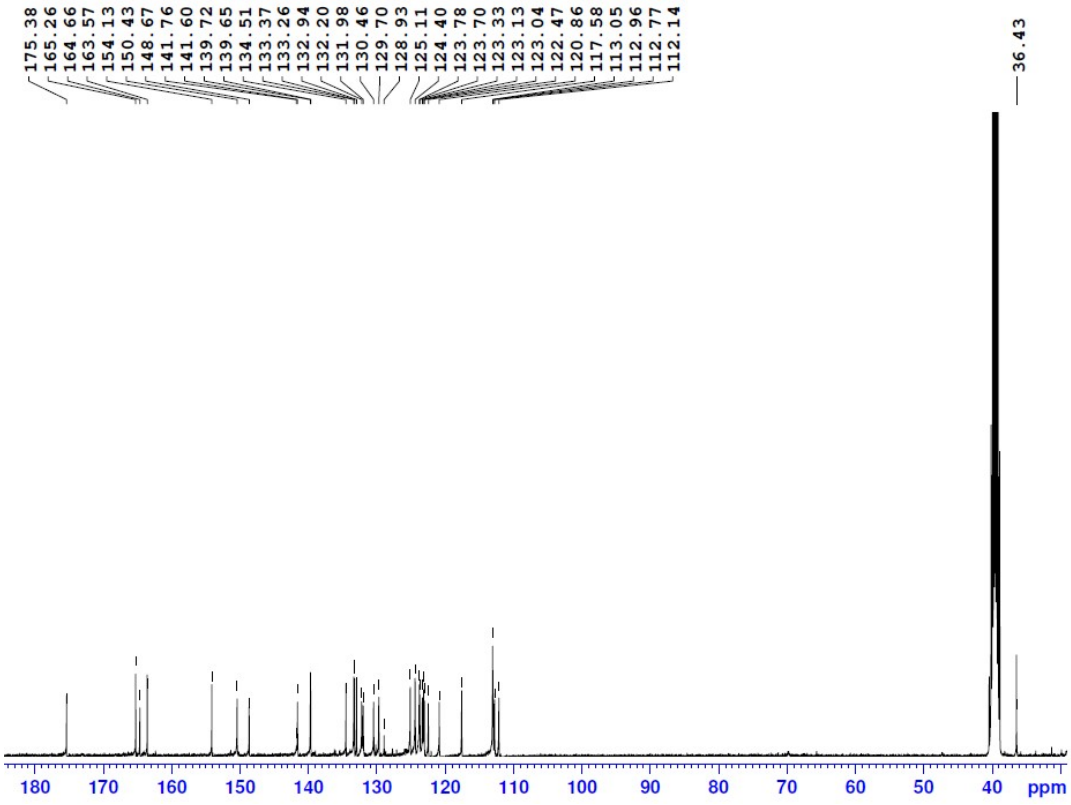

Figure S55. ^{13}C-NMR spectrum for **19** in DMSO.

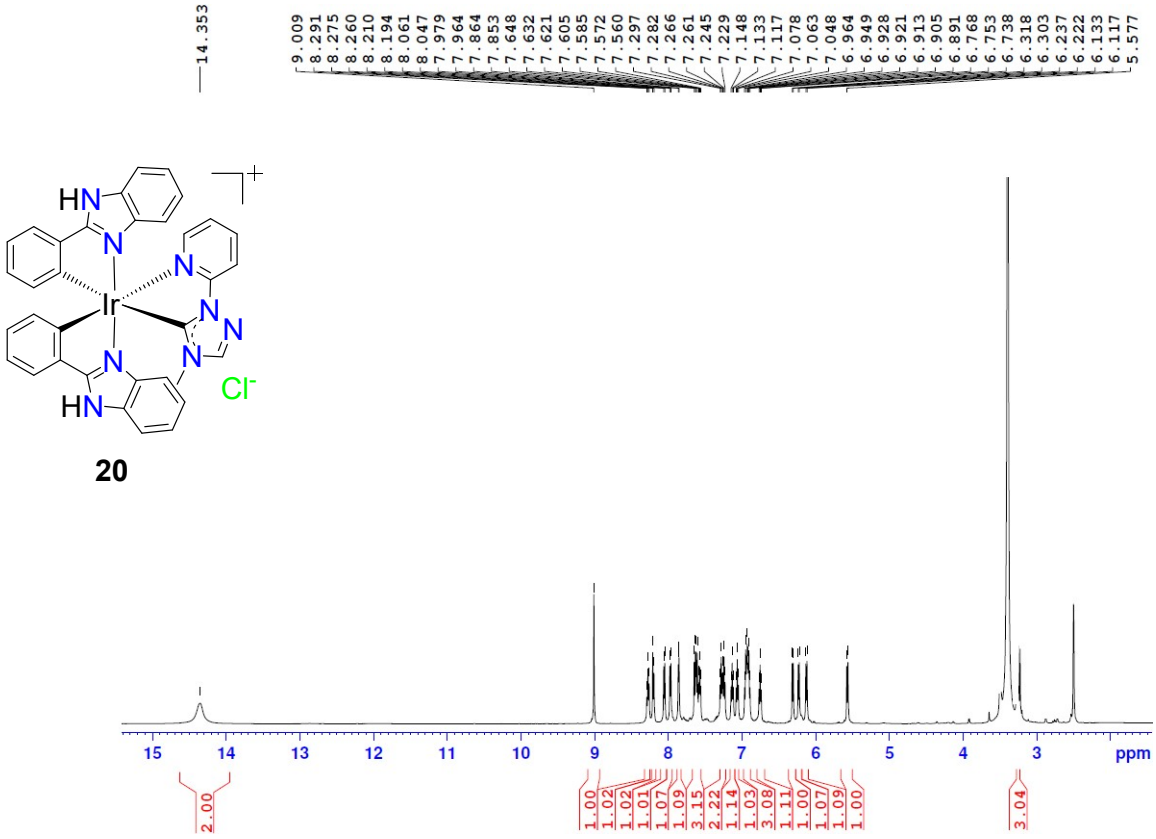

Figure S56. ^{1}H-NMR spectrum for **20** in DMSO.

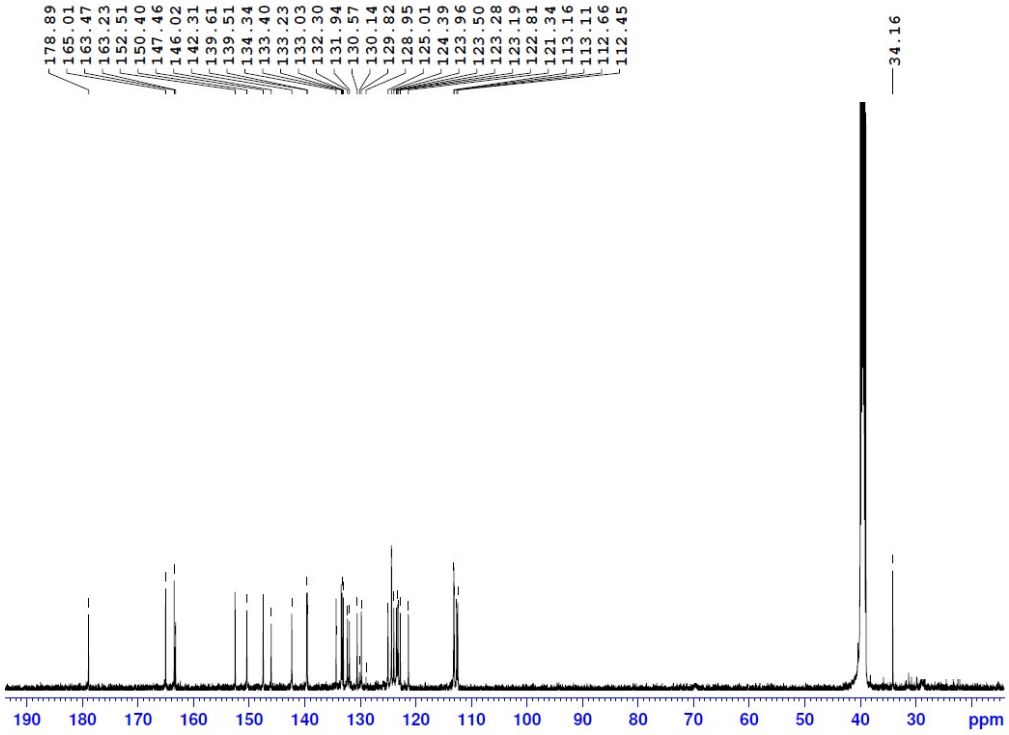

Figure S57. ^{13}C-NMR spectrum for **20** in DMSO.

7. References

1. S. Sprouse, K. King, P. Spellane and R. J. Watts, *J. Am. Chem. Soc.*, 1984, **106**, 6647-6653.
2. L. A. Stott, K. E. Prosser, E. K. Berdichevsky, C. J. Walsby and J. J. Warren, *Chem. Commun.*, 2017, **53**, 651-654.
3. M. S. Kabir, M. Lorenz, O. A. Namjoshi and J. M. Cook, *Org. Lett.*, 2010, **12**, 464-467.
4. R. Schiffmann, A. Neugebauer and C. D. Klein, *J. Med. Chem.*, 2006, **49**, 511-522.
5. H. Zhang, Q. Cai and D. Ma, *J. Org. Chem.*, 2005, **70**, 5164-5173.